REANALYSIS OF CRUCIFORM SPECIMEN FATIGUE RESULTS BY STATISTICAL METHODS

A Thesis

Presented to

the Faculty of the Department of Civil Engineering

The University of Houston

In Partial Fulfillment

of the Requirements for the Degree

Master of Science in Civil Engineering

---

by

Shun-Sheng Yang

August 1975

DEDICATION

To my parents, whose encouragement and expectations were always a source of inspiration.

ACKNOWLEDGMENTS

The writer wishes to express his sincere appreciation to the many individuals whose contributions of time, effort, and encouragement, made this study possible.

Special appreciation is expressed to Dr. William J. Graff, Chairman of the thesis committee, for his expertise, guidance, and encouragement throughout the course of this project and my graduate study here.

Grateful appreciation is expressed to Dr. Ardis H. White, Chairman of the Civil Engineering Department, and to Dr. Kamel Salama from the Mechanical Engineering Department, for serving on the thesis committee.

Sincere thanks are extended to Mr. Bob Pan, and Miss Grace Tung for their assistance and support, which made completion of this thesis possible.

Special acknowledgement is made to Mrs. Jean Graff for her neat and accurate typing of this thesis.

REANALYSIS OF CRUCIFORM SPECIMEN FATIGUE RESULTS BY STATISTICAL METHODS

An Abstract of a Thesis

Presented to

the Faculty of the Department of Civil Engineering

The University of Houston

In Partial Fulfillment

of the Requirements for the Degree

Master of Science in Civil Engineering

---

by

Shun-Sheng Yang

August 1975

ABSTRACT

This thesis brings together the experimental results available in nine published papers spread over thirty-five years in the technical literature. The specimens tested and reported in these papers had sufficient commonality of variables to permit reanalysis of the fatigue results by statistical methods. Through these techniques the original conclusions of the investigators have been reinforced and broadened, that is, made more general for the purposes of the design engineer.

TABLE OF CONTENTS

LIST OF TABLES

LIST OF FIGURES

CHAPTER 1

INTRODUCTION

INTRODUCTION

It is relatively common for a structural member or connection subjected to a cyclically varying load to fail after a certain number of load applications even though the maximum nominal stress per cycle is less than the yield stress of the parent metal or of the weld metal. Such a failure is called a fatigue failure because cracks are initiated at some mechanical or metallurgical stress concentration point in the structure and are propagated through the material with successive load applications until the affected part loses its ability to carry load.

For a ductile metal the fatigue life increases with decrease in maximum stress until the fatigue limit is reached. This limit is defined as the maximum stress level at which 50 percent of the specimens will survive some very large number of cycles, say 5 or 10 million cycles. Whereas fatigue limit implies infinite life at some limiting low or moderate level of stress, fatigue life is the finite cyclic time associated with a stress level higher than that corresponding to infinite life. Such a stress level is called the fatigue strength for that fatigue lifetime.

Although a vast number of investigations have been made over the last 100 years, there is still no analytical method available by which the fatigue strength of a particular member may be predicted for a certain operating lifetime. Instead, it is necessary to conduct fatigue tests on models or prototype parts, and then base final design on the results of such tests.

Fatigue test results are commonly plotted either as maximum stress per cycle versus service life, or stress range per cycle versus service life. These curves, plotted either as semilog or log-log curves are called S-N curves. For example, in terms of maximum stress, the S-N curve that best describes the central tendency of a set of data at a given maximum stress defines the fatigue life for which 50 percent of the specimens may be expected to fail at that stress level.

Fatigue failure has long been recognized as a random process depending in more or less unknown fashion on a number of variables. Factors that contribute to the randomness of fatigue failure are: inhomogenities of metals as represented by variations of mechanical properties from heat to heat and even from bar to bar within a heat; inadequacies in stress calculations; incomplete simulation of real stress level variations; unknown fabrication and residual stresses, and effects of environment.

For many years investigators have resorted to statistical approaches to fatigue data in an effort to reduce randomness and permit drawing of significant results from widely scattered data. Over these years interpretation of experimental data consisted mainly of selecting various stress levels and testing specimens to determine average lifetimes at each stress level. Curves drawn through these average points were considered to be the mean S-N curves. Beginning with ASTM Committee on Fatigue (E-9)(1)* the probability of survival based on measures of dispersion such as percentiles and standard deviation were recognized as more reliable interpretations of fatigue data than the mean S-N curve.

---

* Numbers in parentheses refer to references.

Gurney and Maddox (2) in the past few years have really reawakened the engineering community to the importance of technical reevaluation of existing fatigue information. The techniques of statistical analysis represent powerful tools for reanalysis. Through their use the original conclusions may be reinforced, broadened and generalized to cover many more significant stress situations than can be envisioned by the interpretation of the data of any one paper alone.

In view of the importance of welded connections between tubular members in offshore structures it seems worthwhile to review the literature in search of papers covering experimental work on welded fatigue specimens of cruciform geometry. While there are many forms of cruciform welded specimens treated in the literature, this investigation was restricted to fillet welded connections where the attachments to the main member extended outward from both sides. Such connections may be classified as transverse load-carrying connections when the main plate is interrupted by the attachment and transverse non-load-carrying connection when the attachments are welded directly opposite to one another on the sides of a continuous main member.

Restricting the search to the cruciform specimen types just described, six papers were found for load-carrying connections where the commonality among the variables was sufficiently close that the experimental results could be compiled and analyzed as one set of data. Three papers were found relating to non-load-carrying connections. In all cases the applied loading was axial tension and compression in the main member.

This thesis presents the results of the statistical reanalysis of

the experimental work contained in these nine papers. A corollary purpose of this thesis is to emphasize the potential for restudying existing fatigue data accumulated over the years. The primary obstacle in doing such reevaluation is sifting of the literature and locating a sufficient number of investigations sufficiently close in terms of variables to permit consolidation.

The thesis is arranged in two parts. The first part is on the fatigue behavior and the use of statistical methods to approach the fatigue phenomena; Chapter 2 provides information on the basic fatigue phenomena and statistical nature of fatigue; Chapter 3 presents the mathematical models for fitting the S-N curve; Chapter 4 outlines the statistical techniques used in this study. The second part of the thesis consists of the Appendix which provides background knowledge on fatigue behavior. This information may be of value to those readers who desire more details on the subject.

The writer does not consider the problems dealt with here to be completely solved and believes that the purpose of this thesis will have been achieved if it helps to increase the number of investigations in this field.

CHAPTER 2

BASIC FATIGUE PHENOMENA AND STATISTICAL NATURE OF FATIGUE

A. THE FATIGUE FAILURE CRITERIA

Fatigue fracture occurs with very small strains and transgranular fracture after application of loads smaller than those which cause static failure. Fatigue behavior of a material is usually assessed by testing a number of specimens to find the number of cycles required to cause complete failure. The strict definition of "cycles to failure" varies from one researcher to another and can either be the initiation of a small visible macrocrack or the final fracture of a test specimen. In most past research projects, the criterion of fatigue failure was complete rupture of the specimen. For long fatigue lives the difference in failure definition is irrelevant, but this criterion becomes more important for low cycle fatigue (or short fatigue lives). Crooker (3) reported that for ferrous alloys the salient feature of the S-N curve is the horizontal portion of the curve at long fatigue lives, indicating a fatigue limit stress below which fatigue failures will not occur. Non-ferrous alloys generally do not exhibit a true fatigue limit; however, for most alloys the slope of the S-N curve becomes nearly flat beyond 10^7 cycles of loading. Fisher, et. al. (4) reported that the deflection criterion he used to define failure was based on observations of the initial behavior of the tested specimens. An increase in midspan deflection of 0.020 in. was found to be equivalent to a crack size that was considered to be incipient failure of the beam section. The cracked area was approximately equal to 75 percent of the beam flange area. The crack growth for test beams having this amount of deflection was observed to be extremely rapid.

Trufyakov (5) reported that fatigue cracks in engineering structures

working in low temperature environments will become the nuclei of brittle fracture. Thus he considered the moment at which a fatigue crack reaches dangerous dimensions to be a better criterion for fatigue breakdown than the moment of total failure. Trufyakov proposed that the fatigue crack becomes dangerous upon reaching a depth of 4 mm (0.16 in.) and that this crack size should be taken as the criterion of fatigue failure. These cracks are quite easily located by ultrasonic defectoscope, and they are frequently located effectively in many joints by the paraffin test.

B. The S-N Diagram

The fatigue fracture relationshionship between stress (S) and number of load applications (N) is usually represented graphically by plotting the stress as ordinate and cycles to failure on the abscissa. These curves are commonly referred to as S-N curves.

The S-N curve is frequently approximated by a straight line on a log-log plot for much of its useful range. For the purpose of determination of the mean fatigue limit a semi-log plot is sometimes used. This approach is valied in a practical sense because: (a) very low-cycle failures approach static strength conditions when compensated for rate of load application, and (b) the high-cycle failure range has poor accuracy and is usually avoided because small variations in stress lead to very large changes in fatigue life. One reason for using caution in the high-cycle range is that damage will accumulate at an applied stress below the S-N curve.

The solid line in Figure 1 shows the results of a typical laboratory fatigue test on a steel commonly used in an aerospace structure. With a testing speed of about 1200 cpm, Grover (6)

tentatively divided the fatigue life into three groups.

(a) $0.25 \times 10^{-1} \leqslant N \leqslant 1.2 \times 10^{3}$

(or $1.4 \leqslant N \leqslant 1{,}200$) low cycle lifetime

(b) $1.2 \times 10^{3} \leqslant N \leqslant 1.2 \times 10^{7}$

(or $1{,}200 \leqslant N \leqslant 12{,}000{,}000$) intermediate cycle lifetime

(c) $N > 1.2 \times 10^{7}$

(or $N > 12{,}000{,}000$) high cycle lifetime.

Grover decided that it was almost meaningless to observe lifetimes less than 1,200 cycles and too time-consuming to test to more than 1.2×10^{7} cycles.

An accurate evaluation of cumulative damage in terms of basic fatigue performance is sometimes questionable, even for a simple test, because the basic mechanics of fatigue damage are poorly understood. Freudenthal (7) tentatively divided the effects of cyclic stress amplitudes into three groups:

(1) A high-stress range where $N < 10^{5}$ cycles. The failures in this range are characterized by severe crystal fragmentation and disorientation accompanied by hardening.

(2) A "true" fatigue stress range where $10^{5} < N < 10^{7}$ cycles. The failures in this region are characterized by reversed slip and slip concentration into striations with very little hardening.

(3) A "safe" stress range where $N > 10^{7}$ cycles. In this range there is widely distributed slip, but neither hardening nor substantial microcrack formation occurs.

Yen (8) reported that a complete S-N curve may be divided into two portions: the low-cycle range and the high cycle range. There is no sharp dividing line between the two. Yen arbitrarily proposed that 0

to about 10^3 or 10^4 to be low cycle range; on the other hand, from about 10^3 or 10^4 cycles to 10^7 or higher is high cycle range.

In general, the low cycle fatigue strength is governed by the material tensile strength. Yielding or plastic deformation of the material may markedly affect the stress distribution in the specimen and total deformation will therefore be the summation of both elastic and plastic strain components. Under these circumstances, where fatigue lifetimes are relatively short, it is often more appropriate to consider strain amplitude rather than stress amplitude as the parameter for the ordinate of the S-N diagram.

Yamaguchi, et. al. (9) reported that for low cycle fatigue the S-N diagram is almost parallel to the abscissa axis in the regions of maximum nominal stress higher than 90% of the tensile strength of the material. Here little difference is seen in the fatigue strength of the specimens irrespective of the variations in the size and shape of the specimens. The fracture surfaces are similar to the static failure surface. At the same time a slight necking is observed to have occurred. Fatigue cracks will have initiated at discontinuous parts of the specimens but these will not have propagated throughout the failure.

In most cases where the fracture surface indicates static failure, caution is recommended since fracture might be caused either by static loading ($N = 1/4$ cycle) or by fatigue loading at high stresses. It should be noted that a slight necking (localized reduction in the cross-section area) does not prove that static rupture has occurred. Yamaguchi found that fluctuating tensile loading (with a mean static component) produces a slight necking. It is believed that the plastic deformation in fatigue caused by high stresses and a low number of load

cycles differs little from the plastic deformation prior to and during crack propagation in static tests, and that the appearance of the two fractured areas is very similar.

Generally, extrapolation of the S-N curve to shorter lifetimes is questionable, while to very long lifetimes there is oftentimes not much test data available to justify it. Table 1 (8) shows the differences between low cycle and high cycle fatigue failure.

C. SCATTER

It has long been recognized that scatter or variation in the fatigue life occurs, and that the degree of scatter depends on the material tested, and the stress level used. Fatigue life is scattered in a wide range even under the same stress condition. The scatter band is usually broader at lower stress level than at high stress level. For this reason in constructing the S-N curve it is preferable to test as many specimens as is economically possible. To work with a limited number of specimens the data collector must use his resources to maximum advantage. It may be preferable to test a number of specimens at one or two stress levels which are predetermined from a knowledge of the material and the range of alternating stress over which the material will work in service, rather than to spread them over a larger stress range.

The experimental techniques used to generate S-N curves are usually very carefully controlled to assure uniformity in such factors as specimen geometry, loading, temperature, and alloy composition, and yet at any one load level the test data scatter may range from 10:1 to 100:1. The causes of scatter may be inherent metallurgical features in the metal. It is reasonable to assume that cracking always starts at a

TABLE 1

COMPARISON OF LOW CYCLE AND HIGH CYCLE FATIGUE

	Low-cycle	High-cycle
Internal stresses and strain hardening	High	Low
Net sum of plastic flow	Macro Size	Micro Size
Gross sum of plastic flow	Small	Large
X-ray disorientation	Large	Small
Slip	Coarse (10^3-10^4 A)	Fine (10 A)
Slip plane distortion	Normal	Persistent
Crack Origin	Interior	Surface
Crack path	Along max. shear	Cross max. tensile stress
Fracture	Delayed static	Structure deterioration

stress concentration point where there is a defect due to the material inhomogeneity. There is the temptation to associate the scatter with such defects and conclude that either all defects must be eliminated or that fatigue life cannot be predicted when the defects and their probability of existence are unknown. To date, there is still not any mathematical model that can predict fatigue life accurately.

Weibull (10) assumed that the frequency distribution of fatigue life is approximately log-normal; this means that logarithms of the cycles to failure at a given stress level approximate a normal or Gaussian distribution over a considerable range of lifetimes. Figure 2 (11) shows that at a given stress level the life scatter is normal if the log-scale is used. Both Figure 2 and Figure 3 (11) show that scatter in fatigue life at a given stress level increases as the stress level decreases.

D. P-S-N DIAGRAM

In the past much experimental work was done using a different stress level for each part tested. These data were then plotted on an S-N diagram and a "best fit" line was drawn through the data points using the least square fitting method. This line represented the mean life that was expected at any stress level. On the other hand, if similar procedures are carried out for many stress levels, a family of S-N curves representing different constant probabilities of failure can be derived. Such curves have become known as probability S-N curves or P-S-N curves. A typical example is shown in Figure 4 (1).

With the use of P-S-N curves, the prediction of fatigue life should become more meaningful. The P-S-N curve can be used to determine the expected life of components where some of the stress cycles exceed the

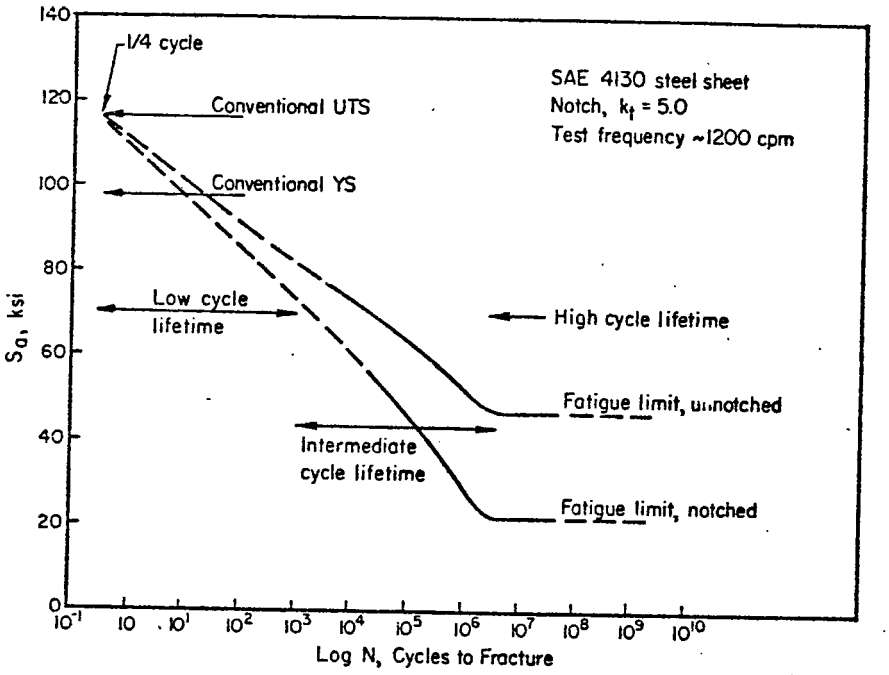

FIGURE 1 RESULTS OF A CONVENTIONAL LABORATORY FATIGUE TEST. (6)

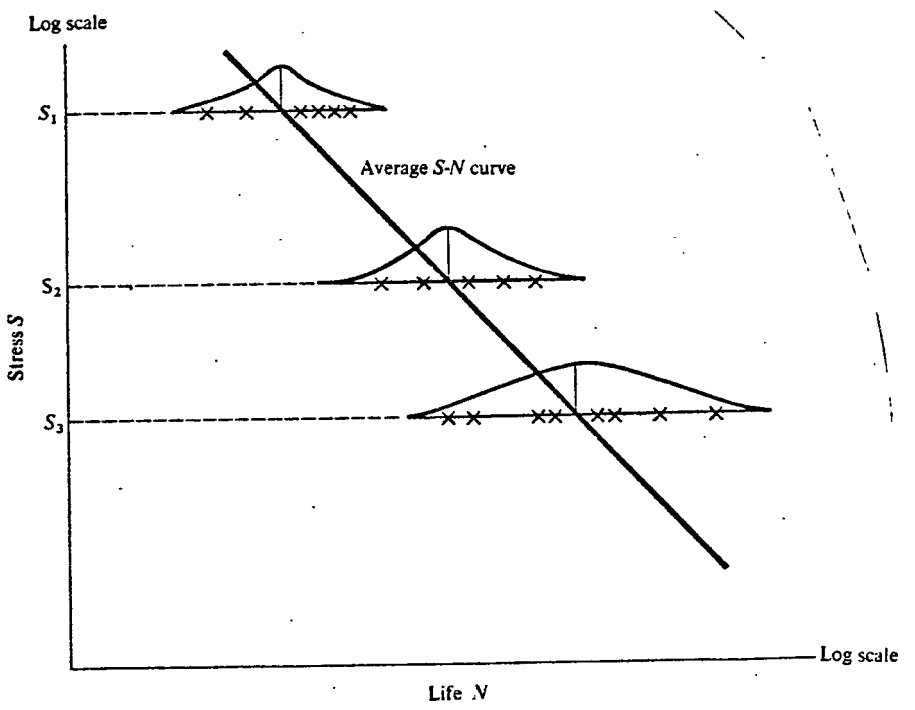

FIGURE 2 SCATTER IN FATIGUE LIFE AT A GIVEN STRESS. (11)

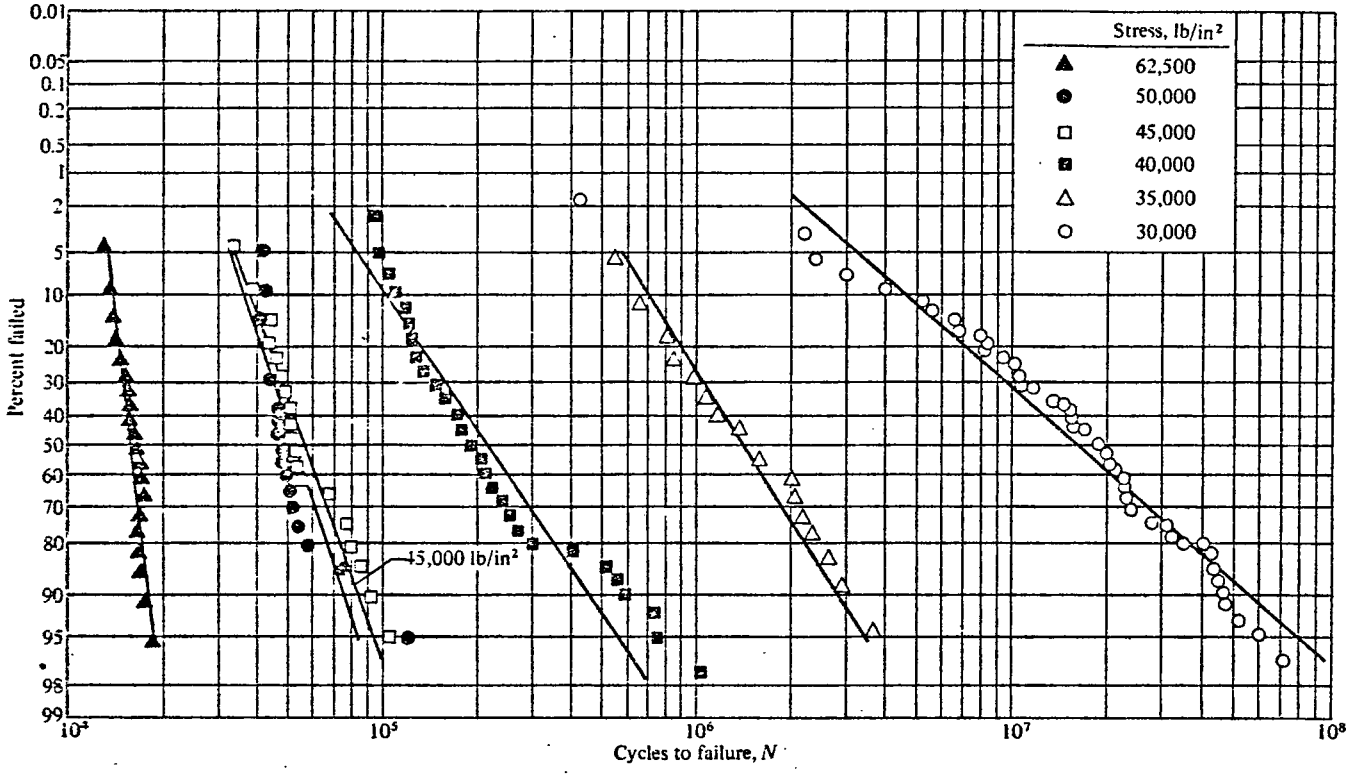

FIGURE 3 LOGARITHMIC NORMAL PROBABILITY PLOT SHOWING INCREASING SCATTER IN LIFE WITH DECRESING STRESS LEVELS. (11)

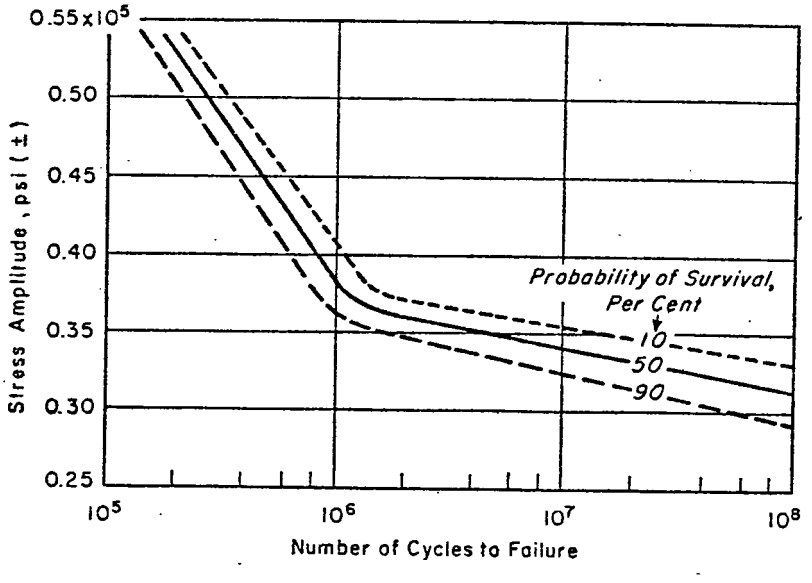

FIGURE 4 PROBABILITY-STRESS-CYCLE (P-S-N) CURVE FOR PHOSPHER-BRONZE STRIP (1)

fatigue limit. The determination of "safe life" can then be related to an acceptable probability of failure and the designer may select a design life based on an appropriate probability of failure and not on an arbitrarily selected factor such as mean endurance or lifetime. Unless otherwise specified, it is generally understood that fatigue information should be interpreted to be the S-N curve for 50 percent survival.

At stress levels around the ordinary fatigue limit the P-S-N curves have the following characteristics in contrast to the customary S-N curves.

(1) The P-S-N curves do not become horizontal, but decrease even at stress levels below the ordinary fatigue limit.

(2) The P-S-N curves turn somewhat toward the left at stress levels around the ordinary fatigue limit.

(3) Fatigue failures at stress levels around the ordinary fatigue limit can be classified into three groups: (a) failure with numbers of cycles corresponding to the lower knee of the S-N curve, (b) failure at lifetimes between that corresponding to the lower knee and 10^8 cycles, (c) and those with numbers of cycles close to 10^8. Moreover, there are specimens which do not fail even at 10^8 cycles.

While not so widely used, fatigue life estimation based on sufficient statistical data and using the probability of survival is much more reliable than the ordinary S-N curve based only on the average value of fatigue life.

CHAPTER 3

MATHEMATICAL MODELS FOR FITTING S-N CURVE

Articles dealing with the mathematical models that have been used to fit the fatigue S-N curve either in log-log form or in semi-log form were reviewed as part of this project. The two categories of models are discussed on the following pages under these headings:

A. Logarithmic mathematical model (log-log S-N plot)

B. Semi-logarithmic mathematical model (Semi-log S-N plot)

A. <u>Logarithmic mathematical model</u> (or power function).

(1) Functional form: $N S^b = a$

Broch (12) reported that for many engineering materials it is possible to approximate the "dangerous part" of the S-N curve by means of an expression of the type

$$N S^b = a \qquad (1)$$

where N is the number of cycles to failure at the stress level S, and a and b are constants which depend upon the material. For common engineering materials b takes values between 3 and 8. For steel b is approximately 3.5.

Upon taking the logarithm of both sides of Equation (1)

$$\log N + b \log S = \log a \qquad (2)$$

$$\log N = \log a - b \log S \qquad (2a)$$

where: $a > 0$, $b > 0$, $a \neq 0$

On the log-log S-N plot, log a is the intercept with x-axis (or abscissa) while b is the slope of the S-N curve. Thus the coefficient a should be greater than zero (i.e., $a > 0$), and should not be equal to zero (i.e., $a \neq 0$), by the definition of a logarithm. Since fatigue stress and cycles to failure are reversely proportional to each other, the fatigue slope b should be negative

If fatigue stress s is to be the independent variable and fatigue life N is to be the dependent variable, then Equation (1) can be expressed in the form:

$$N = a S^{-b} \tag{3}$$

Two of the simplest cases of Equation (3) are Equation (4) and Equation (5), in which $a = 1$ for both equations, while on the other hand, $b = -2$ and $b = -3$, respectively.

$$N = S^{-2} = \frac{1}{S^2} \qquad (a = 1,\ b = -2) \tag{4}$$

and

$$N = S^{-3} = \frac{1}{S^3} \qquad (a = 1,\ b = -3) \tag{5}$$

The concepts used in Tables 2 and 3 and in Figure 5 do not represent the real fatigue phenomenon. In real fatigue testing, say for a stress $S = 60$ ksi, a value of $b = 3$, and $N = 10^7$, Equation (2) can be shown as follows:

$$\log a = \log (10^7) + 3 \log (60)$$

$$\log a = 8 + 5.3345 = 13.3345$$

$$a = 2.16 \times 10^{13}$$

Thus it is seen that the coefficient $a = 2.16 \times 10^{13}$ is much larger than the assumed value $a = 1$ in Equation (5). In fact, this constant a can be treated as a magnification factor. It is obvious when the model $N = a S^{-b}$ $(a > 1)$ is used that all the tabulated values in Table 2 and Table 3 should be multiplied by a magnification factor "a".

Practically, in order to determine the finite life region of the S-N curve, the model $N S^b = a$ may be described mathematically by regression analysis. The method of least squares can be used to fit the

TABLE 2

SUBSTITUTION OF NUMBERS IN EQUATION 4

	Compression								Tension						
S	$-\infty$	---	-5	-4	-3	-2	-1	0	1	2	3	4	5	---	$+\infty$
N	0	---	0.04	0.065	0.11	0.25	1	$+\infty$	1	0.25	0.11	0.065	0.04	---	0

TABLE 3

SUBSTITUTION OF NUMBERS IN EQUATION 5

	Negative cycles are meaningless	Tension							
S		0	1	2	3	4	5	---	$+\infty$
N		$+\infty$	1	0.125	0.031	0.0156	0.008	---	0

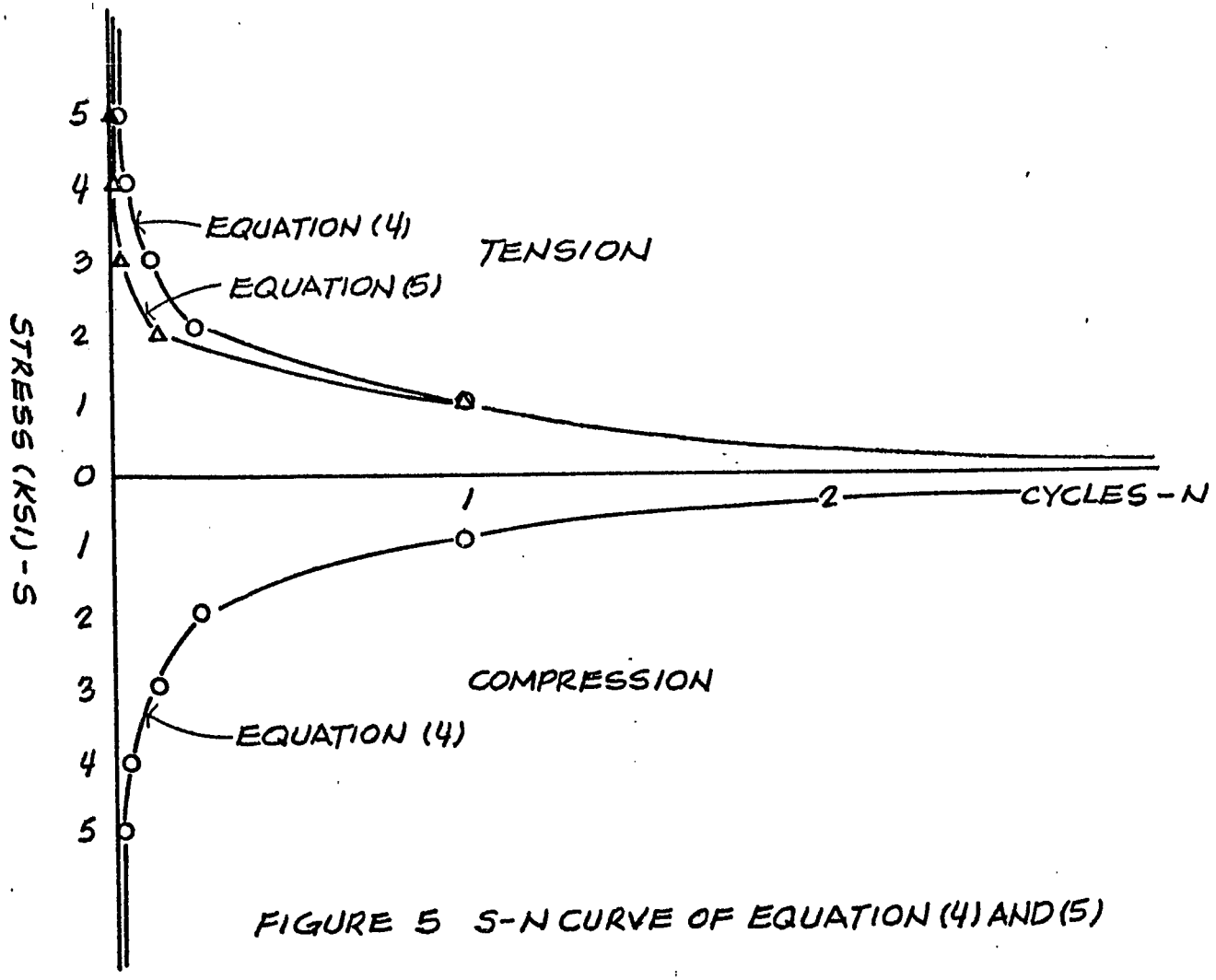

FIGURE 5 S-N CURVE OF EQUATION (4) AND (5)

linear equation, $y = B_0 + B_1 x$, to the data. Comparing Equation (2a) with the linear equation $y = B_0 + B_1 x$, the linear transformation pairs can be shown as follows:

$$\begin{aligned} \log a &= B_0 \\ -b &= B_1 \\ \log N &= y \\ \log S &= x \end{aligned} \qquad (6)$$

Past experience indicates that this type of power function can be fitted well to fatigue test data only in the cycle range from 10^3 or 10^4 to 10^7 (i.e., the finite fatigue life range) and for intermediate stress levels. Use of this power function for very high stress levels, low stress levels and the stress level around the fatigue limit is still questionable. It is expected that these problems will be solved in future studies.

In ordinary fatigue testing where $a > 1$, the value of a varies a great deal from one material to another. On the other hand, for the coefficient b (i.e., the slope of the S-N curve) is almost fixed. Fisher (4) suggested that a good fit to the fatigue data from his investigation could be obtained by letting the constant b have the value of 3. As mentioned at the beginning of this chapter, Broch (12) indicated that for steel b is approximately equal to 3.5. Moses (13) indicated that for fatigue design of highway bridge girders it can be reasonably assumed that the fatigue S-N curve, plotted as stress range versus the number of cycles to failure, is a straight line on log-log paper with essentially the same slope, $b = 3$, regardless of the type of steel or the type of weld.

(2) Functional form: $N = a S^b$

This type of equation was suggested by Reemsnyder (14).

$$N = a S^b \tag{7}$$

By taking the logarithm at both sides of Equation (7)

$$\log N = \log a + b \log S \tag{8}$$

In Equation (8)

$$\begin{aligned} a &> 0 \\ a &\neq 0 \\ b &< 0 \end{aligned} \tag{8a}$$

This is actually the same S-N relationship as in Equation (1), except that here b should be less than zero.

The original logarithmic equation proposed by Reemsnyder (14) is as follows:

$$N = G S^B \quad (\text{where } G = \log^{-1} A)$$

Rewriting: $N = (\log^{-1} A) S^B$

and $\log N = \log (\log^{-1} A) + B \log S$

In this case let

$$\log a = A \quad \text{and}$$

$$b = B \tag{9}$$

This becomes the same S-N relationship as in Equations (8) and (7).

(3) Functional form: $S = a_0 N^{-b_0}$

A different type of power function is found in most of the Japanese literature, namely

$$S = a_0 N^{-b_0} \tag{10}$$

A typical example was indicated by Takahashi (15).

The logarithmic form of Equation (10) is:

$$\log S = \log a_0 - b_0 \log N \tag{11}$$

$$b_0 \log N = \log a_0 - \log S \tag{11a}$$

$$\log N = (1/b_0) \log a_0 - (1/b_0) \log S \tag{11b}$$

where:

$$b_0 > 0$$

$$a_0 > 0 \tag{11c}$$

$$a_0 \neq 0$$

In this case let

$$\log a = (1/b_0) \log A_0$$

$$\text{and} \quad b = (1\ b_0) \tag{12}$$

This becomes the same S-N relationship as in Equations (2) and (11).

But a different nomenclature was used in Takahashi's paper; it is advisable to display the original equation as follows:

$$= b_0 \ N^{-A'}$$

$$\log = -A' \log N + \log b_0$$

$$A' \log N = \log b_0 - \log \sigma$$

$$\log N = \left(\frac{1}{A'}\right) \log b_0 - \left(\frac{1}{A'}\right) \log$$

In this case let

$$\log a = \frac{1}{A'} \log b_0$$

$$\text{and} \quad b = \frac{1}{A'} \tag{13}$$

$$\text{and} \quad S = \sigma$$

This becomes exactly the same S-N relationship as in Equations (1) and (2). This type of power function can be seen in Japanese literature quite often. It was probably proposed first by T. Yokobori.

In fact, all of the three previous types of power functions prove to be exactly the same thing, except that: in type (1), $b > 0$ and $a > 0$; in type (2), $b < 0$ and $a > 0$; and in type (3), $b_0 > 0$

and $a_c > 0$.

Some other types of expressions with minor differences may be described briefly as follows:

(i) White (16)

$$N (S - So)^{\alpha} = C \qquad (14)$$

where N = number of cycles at which failure occurs under uniform amplitude S

C, So = constant in equation fitted to S-N results

α = exponent in equation fitted to S-N results

Some expressions contain, in addition, a statement of the fatigue limit S_f, or ultimate tensile stress S_u.

(ii) Fisher, B. C. (17)

$$\frac{S - S_f}{S_u - S} = a N^{-b} \qquad (15)$$

or $$\log \left(\frac{S - S_f}{S_u - S} \right) = - b \log N + \log a$$

(iii) Reemsnyder (14)

$$N = E (S - S_f)^B \qquad (16)$$

or $$\log N = A + B \log (S - S_f)$$

where $E = \log^{-1} A$

When it is of interest to consider changes in N with changes in S, then

$$N_i = N_o \left(\frac{S_o}{S_i} \right)^b \qquad (17)$$

where the subscript o refers to a known point on the S-N curve and the

subscript i represents the conditions related to or resulting from load i.

(iv) Manse (18)

$$F_n = S \left(\frac{N}{n} \right)^K \tag{18}$$

where F_n = the fatigue strength computed for failure at n cycles

S = the stress which produced failure in N cycles

K = the slope of the best-fit straight line representing the data

(v) SAE Fatigue Design Handbook (19)

$$N = C \; S^{-1/a} \tag{19}$$

where N = cycles to failure

S = stress level

a = slope of S-N curve

C = constant for a given curve

Taking the ratio of two points on the curve, the following can be obtained:

$$\frac{N_1}{N_2} = \frac{C \; S_1^{-1/a}}{C \; S_2^{-1/a}} = \left(\frac{S_2}{S_1} \right)^{1/a} = \left(\frac{S_2}{S_1} \right)^{d} \tag{20}$$

where d = inverse slope of the S-N curve

B. <u>Semi-logarithmic Mathematical Model</u>

(1) Funtional form: $\log N = A + B S$

The semi-logarithmic mathematical model proposed by Reemsnyder is:

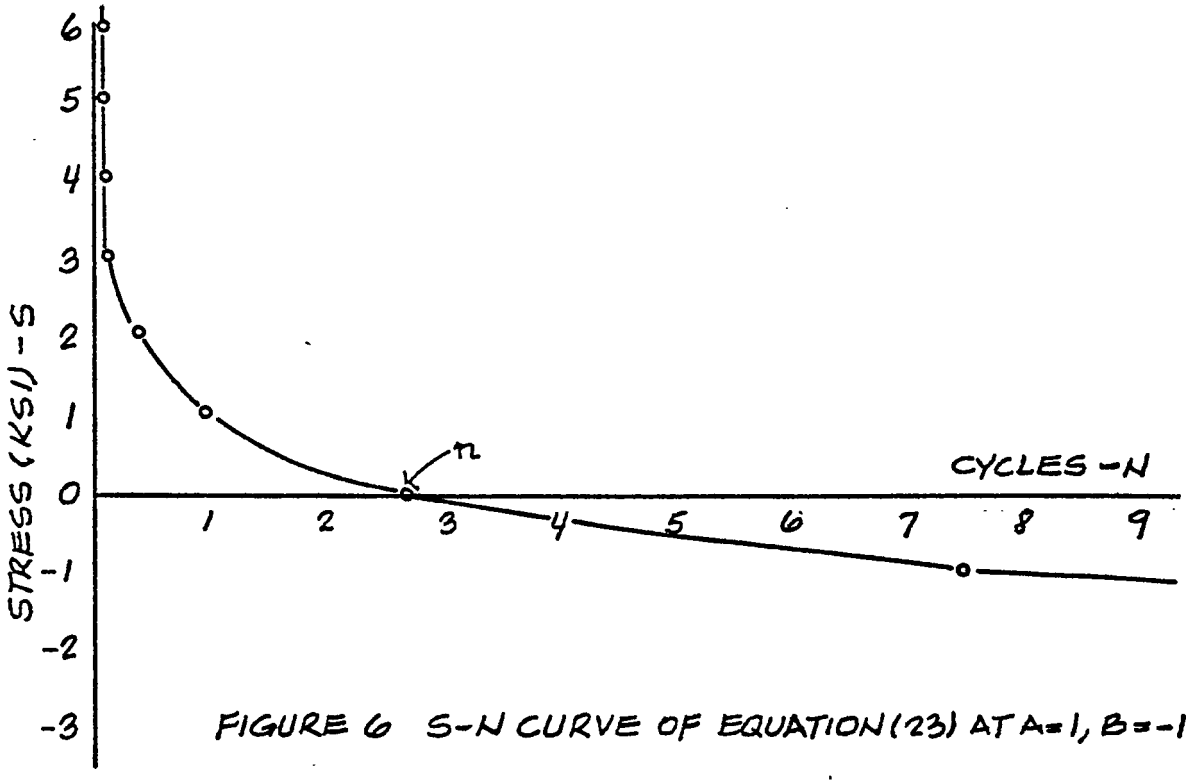

FIGURE 6 S-N CURVE OF EQUATION (23) AT A=1, B=-1

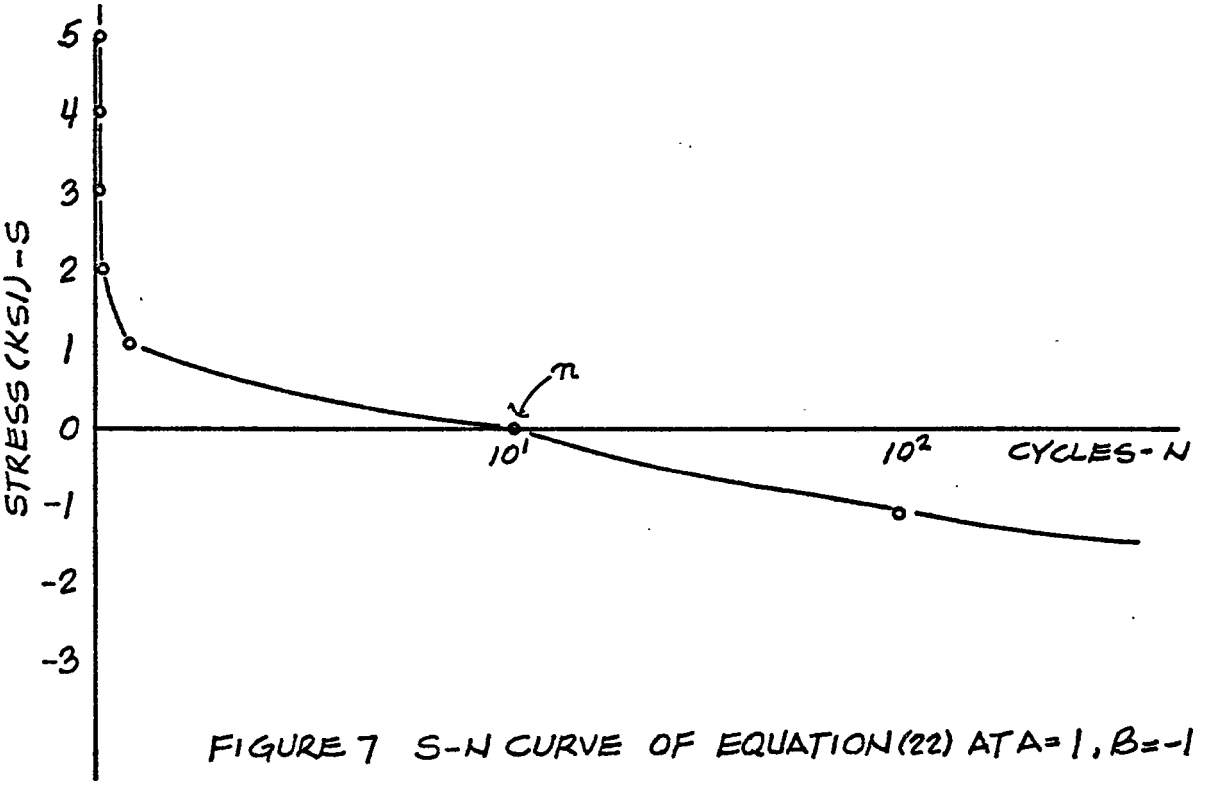

FIGURE 7 S-N CURVE OF EQUATION (22) AT A=1, B=-1

$$\log N = A + B S \tag{21}$$

Alternatively,

$$N = 10^{(A + B S)} \tag{22}$$

if the common logarithm base is used

and

$$N = e^{(A + B S)} \tag{23}$$

if the natural logarithm base is used

Equation (23) can be rewritten as:

$$N = e^{A} \cdot e^{B S} \tag{23a}$$

One special case is: $A = 1$, and $B = -1$. Then Equation (23) becomes

$$N = e \cdot e^{-S}$$

or

$$N = e^{-S + 1} \tag{23b}$$

TABLE 4

SUBSTITUTION OF NUMBERS IN EQUATION 23b

S	-3	-2	-1	0	1	2	3	4	5	6	---	$+\infty$
N	54.60	20.09	7.39	2.72	1	0.368	0.135	0.050	0.013	0.0067	---	0

In Table 4, as the stress level increases, the value of N will approach zero very rapidly. On the other hand, the value of N will not approach infinity as the stress level decreases to zero. One important characteristic of this type of curve is that coefficient A increases while coefficient B is still equal to - 1; the intercept point n will move to the right very rapidly (i.e., the value of n will increase rapidly). Point n is shown in Figure 6.

If the logarithm base is 10, then Equation (22) can be rewirtten as:

$$N = 10^{A} \cdot 10^{B S} \tag{22a}$$

Letting $A = 1$ and $B = -1$, Equation (22) becomes

$$N = 10 \cdot 10^{-S}$$

or

$$N = 10^{-S+1} \qquad (22b)$$

TABLE 5

SUBSTITUTION OF NUMBERS IN EQUATION 22b

S	-3	-2	-1	0	1	2	3	4	5	6	---	$+\infty$
N	10^4	10^3	10^2	10	1	10^{-1}	10^{-2}	10^{-3}	10^{-4}	10^{-5}	---	0

When the common logarithmic model is used the value of n (intercept with x-axis) will move more rapidly to the right than when the natural logarithmic model is used. The common logarithmic model has a curve similar to that of the natural logarithmic model. The advantage of using the common logarithmic model is that the intercept n moves to the right along the x-axis more rapidly. The common logarithmic model speed is about 3.68 (10/2.71828) times faster than that for the natural logarithmic model. This is probably the reason Reemsnyder (14) prefers the common logarithmic model.

It is essential to note that the model can not be used without stating the corresponding value of A and B. In this case the fitted constant A should be positive (i.e., $A > 0$), and constant B should be negative (i.e., $B < 0$).

(2) Functional form: $\log N = a - b S$

In the Japanese literature the model form $\sigma = A' \log N + B'$ (15) is used, in which σ is stress, and N is cycles to failure. In the present thesis this stress symbol σ is replaced by the stress

symbol S.

$$S = -A' \log N + B' \tag{24}$$

$$A' \log N = B' - S$$

$$\log N = \left(\frac{B'}{A'}\right) - \left(\frac{1}{A'}\right) S \tag{25}$$

Comparing with Equation (21) in the previous section

$$\frac{B'}{A'} = A > 0 \tag{26a}$$

$$\frac{-1}{A'} = B < 0 \tag{26b}$$

From the definition of the previous logarithmic model it is known that $A > 0$ and $B < 0$. It is obvious in Equation (26a) that B' and A' should have the same sign, that means the same sign for both denominator or numerator. From Equation (26b) it may be noted that constant A' should be positive. Thus

$$\begin{aligned} A' &> 0 \\ B' &> 0 \end{aligned} \tag{27}$$

Fisher (4) reported some other types of semi-logarithmic mathematical models which came originally from Basquin (20). These have different definitions of the stress variable.

$$\log N = B_1 + B_2 S_r \tag{28}$$

$$\log N = B_1 + B_2 S_{max} \tag{29}$$

$$\log N = B_1 + B_2 S_r + B_3 S_{min} \tag{30}$$

in which S_r = stress range

S_{max} = peak stress

S_{min} = minimum stress

B_1, B_2, B_3 are all constants fitted to the S-log N test results.

CHAPTER 4

STATISTICAL RE-EVALUATION OF TWO WELDED CRUCIFORM JOINTS

A. GENERAL CONSIDERATIONS

Experiments over many years have revealed a significant amount of scatter in fatigue test results even when the same stress level was used for each test. When the scatter is great it is not easy to interpret useful information from the data, and it is even doubtful whether the mean value has any significance. For this reason researchers began using statistical interpretation of fatigue data two or three decades ago.

Although statistical design of experiments is well known to statisticians, the use of these techniques in the planning and evaluation of fatigue results has received wide recognition only during the last ten or fifteen years. These statistical methods point the way towards the most efficient utilization of available literature from earlier investigations.

Gurney and Maddox (2) have in the past few years reawakened the engineering community to the importance of technical reevaluation of existing fatigue information. The techniques of statistical analysis represent powerful tools for reanalysis. Through their use the original conclusions may be reinforced, broadened and generalized to cover more significant stress situations than can be envisioned by the interpretation of the data of any one paper alone.

In view of the importance of welded connections between tubular members in offshore structures it seems worthwhile to review the literature in search of papers covering experimental work on welded fatigue specimens of cruciform geometry. While there are many forms of cruciform welded specimens treated in the literature, this investigation

is restricted to fillet welded connections where attachments to the main member extend outward from both sides as shown in Figure 8. Such connections may be classified as transverse load-carrying when the main plate is interrupted by the attachments and transverse non-load-carrying when the attachments are welded directly opposite to one another on the sides of a continuous main member.

Restricting the search to the cruciform types just described, six papers were found for load-carrying connections where the commonality among variables was sufficiently close that the experimental results could be compiled and analyzed together. Three papers were found relating to non-load-carrying connections. In all cases the applied loading was axial tension and compression in the main member.

B. STATISTICAL TECHNIQUES

Fatigue data plotted as S-N curves are usually interpreted in three regions: high stress - low cycle region, finite life region, and low stress - high cycle region. In this thesis only a portion of the intermediate or finite life region, namely from 1×10^5 cycles to 2×10^6 cycles, is considered. This interval was dictated by the ranges of lifetimes used in the original investigations.

This reanalysis has centered on the evaluation of the effect of the following variables:

A. For the transverse load-carrying joints:

1. Central block width (w); also called attachment width
2. Length of weld (L)
3. Main plate thickness (t)
4. Fillet weld size (S)

B. For the transverse non-load carrying joints:

1. Attachment width (w)
2. Fillet weld size (S)
3. Length of weld (L)

The statistical analysis was carried out using the UNIVAC 1108 computer at the Computing Center of the University of Houston. The program provided the following output as standard for all runs:

a. Listing of input data.
b. Means and standard deviations for each input variable.
c. Simple (Pearson's Product-Moment) correlation coefficients between all input variables.
d. The ordinary least squares estimates of regression coefficients.
e. The standard error of each coefficient estimated.
f. An analysis of variance table for regression.
g. The value of R^2.
h. A listing of the values of observed dependent variable and predicted dependent variable for each model.

For the linear regression analysis throughout the investigation four basic empirical models were used:

Model I : $\text{Log}(N) = B_0 + B_1 (S_R)$

Model II : $\text{Log}(N) = B_0 + B_1 \text{Log}(S_R)$

Model III: $\text{Log}(N) = B_0 + B_1 (S_{max})$

Model IV : $\text{Log}(N) = B_0 + B_1 \text{Log}(S_{max})$

in which B_1 = regression coefficient

B_0 = constant term for fitted regression curve

$\text{Log}(N)$ = the dependent variable

S_R , S_{max}, $\text{Log}(S_R)$, $\text{Log}(S_{max})$ = independent variables

S_R, S_{max} = stress range and maximum stress, respectively

Log (S_R), Log (S_{max}) = Log - transformed stress range and maximum stress, respectively

C. TRANSVERSE LOAD-CARRYING CRUCIFORM SPECIMENS

Six papers were reviewed. The fatigue strength of this type of joint depends mainly on four variables. As shown in Figures 8(a) and 8(b) they are: fillet weld size (S), main plate thickness (t), central block width (w), and length of weld (L).

(1) The effect of central block width.

The other three variables were kept at constant levels while the central block width was permitted to vary. Only two papers of the six qualified in this category (21, 22). The variables are listed in Table 6.

Two separate regression lines were fitted to the finite-life data from References No. 21 and 22 using the logarithm of the number of cycles to failure (log N) as the dependent variable, and stress range (S_R), or logarithm of stress range (Log (S_R)), as the two independent variables. Note that for zero-to-tension loading: $S = S_R = S_{max.}$, and Log (S) = Log (S_R) = Log ($S_{max.}$).

Through the method of least squares using the computer, mean regression lines represented by the following equations were determined. The standard error of estimate varied from 0.201 to 0.232 for Reference 21, and from 0.273 to 0.333 for Reference 22. The correlation coefficient for each equation is shown in Figures 9, 10 and 11.

In Figure 9 the semilog plot shows Models I and III to be:

$$\text{Log (N)} = 7.36240 - 0.12098 \text{ (S)} \qquad (31)$$

The log-log ordinate shows Models II and IV to be:

TABLE 6

VARIABLES OF THE TRANSVERSE LOAD-CARRYING CRUCIFORM JOINTS

Ref. No.	Original Specimen Designation	Fillet Weld Size (in.) S	Main Plate Thickness (in.) t	Central Block width (in.) w	Length of weld (in.) L	Stress Ratio R
21		0.3125"	0.75"	0.875"	4"	0
22		0.3125"	0.75	0.75"	4"	0
23	Series 1	0.378"	0.75"	0.75"	1.18"	-1
	2	0.37"	0.75"	0.75"	1.18"	-1
	3	0.33"	0.75"	0.75"	1.18"	-1
	4	0.34"	0.75"	0.75"	1.18"	-1
	5	0.33	0.75"	0.75"	1.18"	0
	6	0.48"	0.625"	0.625"	1.18"	-1
	7	0.48"	0.625"	0.625"	1.18"	-1
24	TTN 1	0.3125"	0.5"	1.25"	4"	0
	TTN 2	0.5"	0.5"	1.5"	4"	0
	TTN 3	0.5"	0.3125"	1.5"	4"	0
27	b = 0	0.39"	0.63"	0.63"	2.36"	0
	b = 0	0.71"	0.63"	0.63"	2.36"	0
	b = $\frac{1}{2}$S	0.35"	0.63"	0.63"	2.36"	0
	b = $\frac{1}{2}$S	0.55"	0.63"	0.63"	2.36"	0
	b = S	0.20"	0.63"	0.63"	2.36"	0
	b = S	0.28"	0.63"	0.63"	2.36"	0
28	b = S (Type A)	0.21"	0.394"	0.394"	2.36"	0
	b = $\frac{1}{2}$S (Type B)	0.27"	0.394"	0.394"	2.36"	0

See Figure labeled "Table 6 Note" for beveling of main plate.

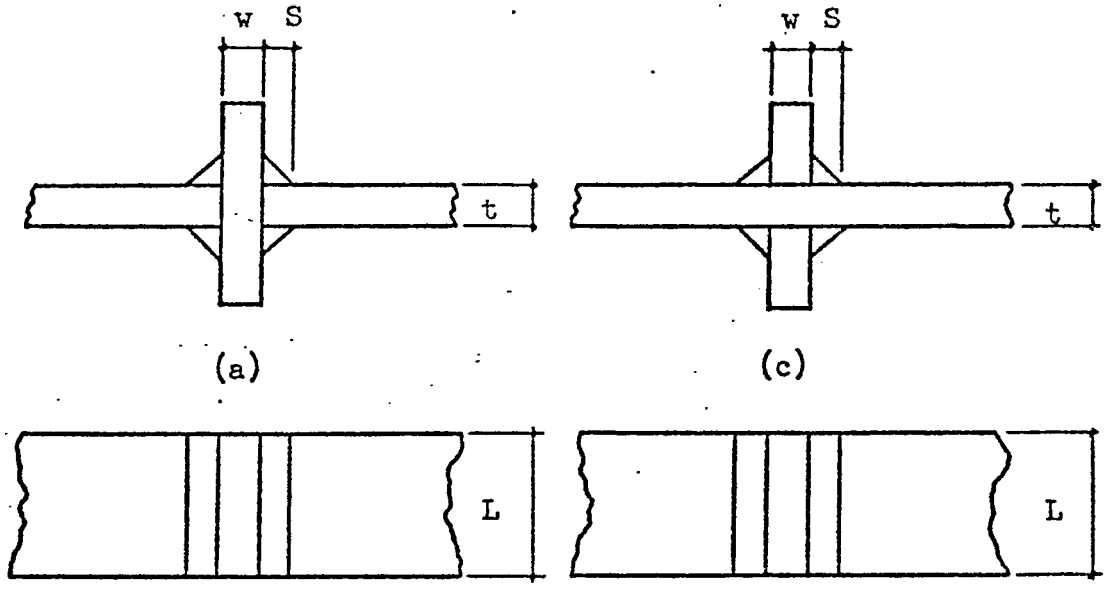

FIGURE 8 FILLET WELDED CRUCIFORM SPECIMENS VIEWS (a) AND (b) REPRESENT THE TRANSVERSE LOAD-CARRYING JOINTS ; VIEWS (c) AND (d) REPRESENT THE TRANSVERSE NON-LOAD-CARRYING JOINTS.

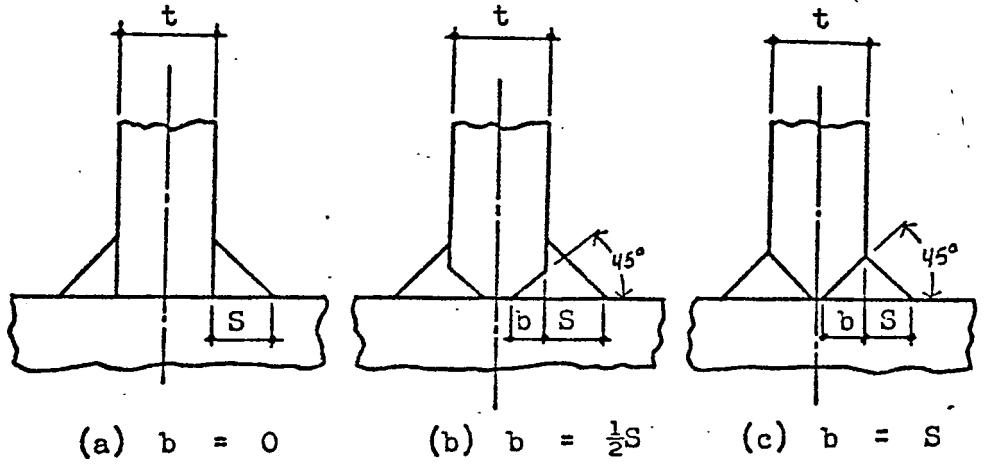

FIGURE TABLE 6 NOTE

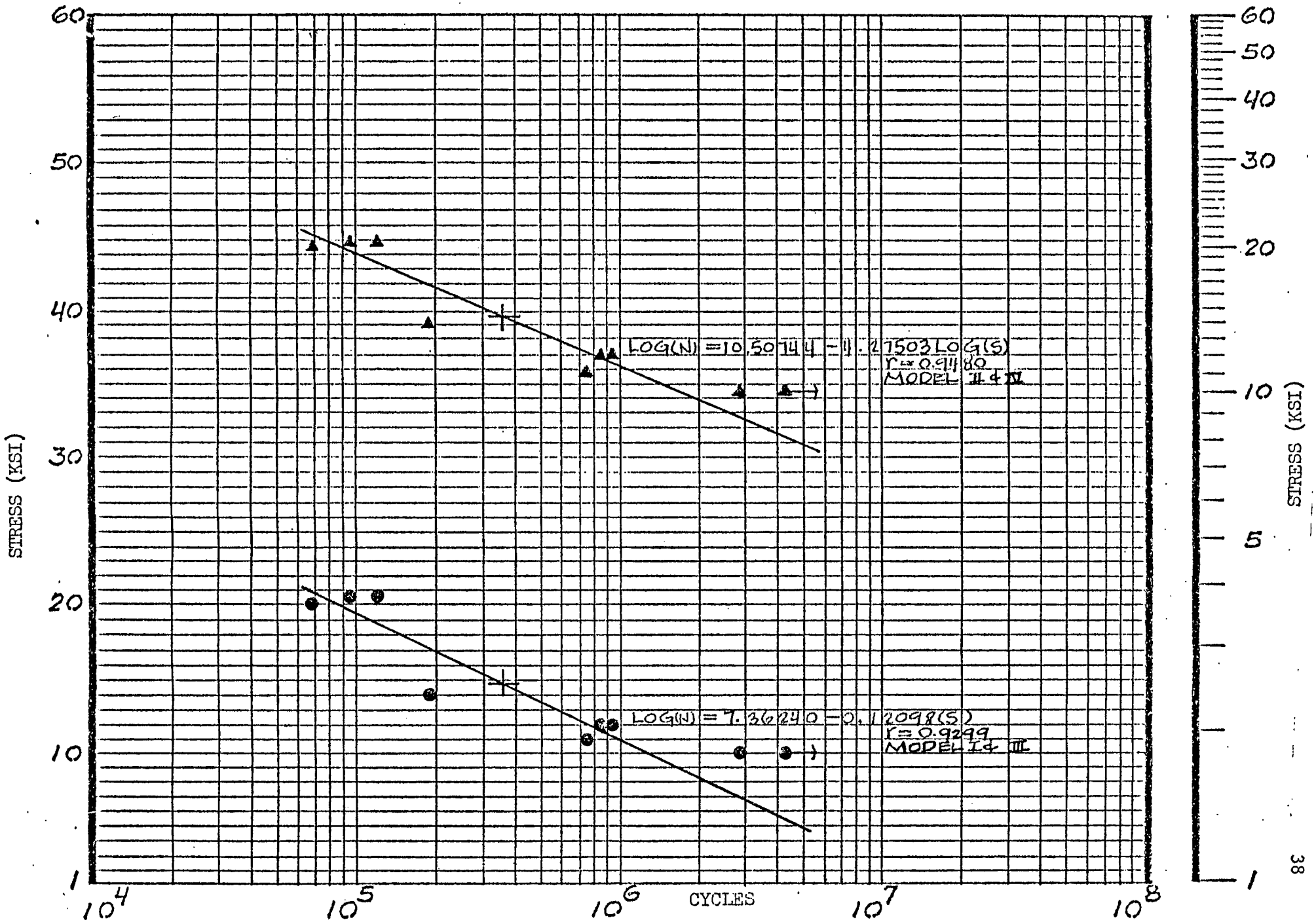

FIGURE 9 REGRESSION ANALYSIS OF REFERENCE 21

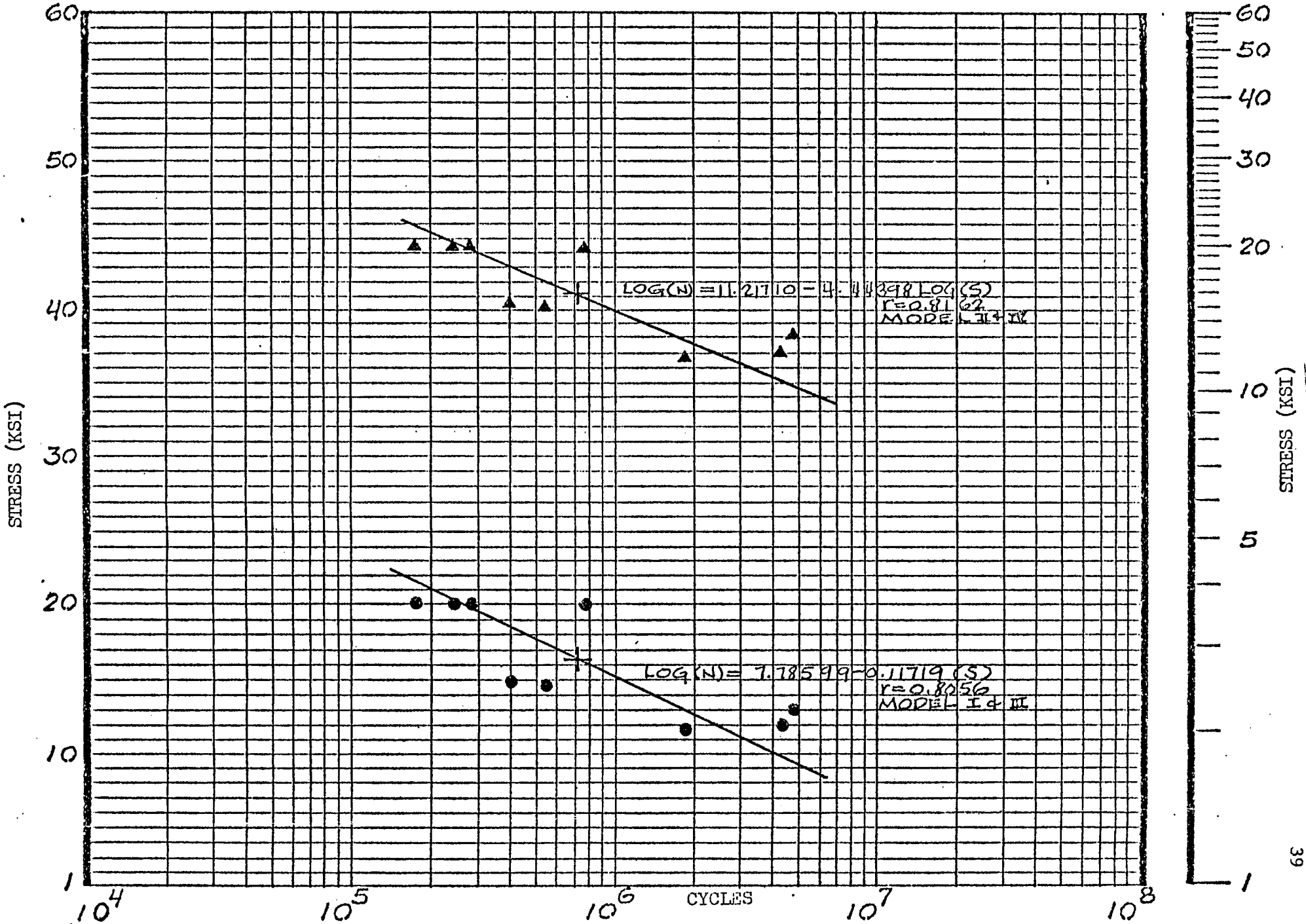

FIGURE 10 REGRESSION ANALYSIS FOR THE A-7 STEEL OF REFERENCE 22

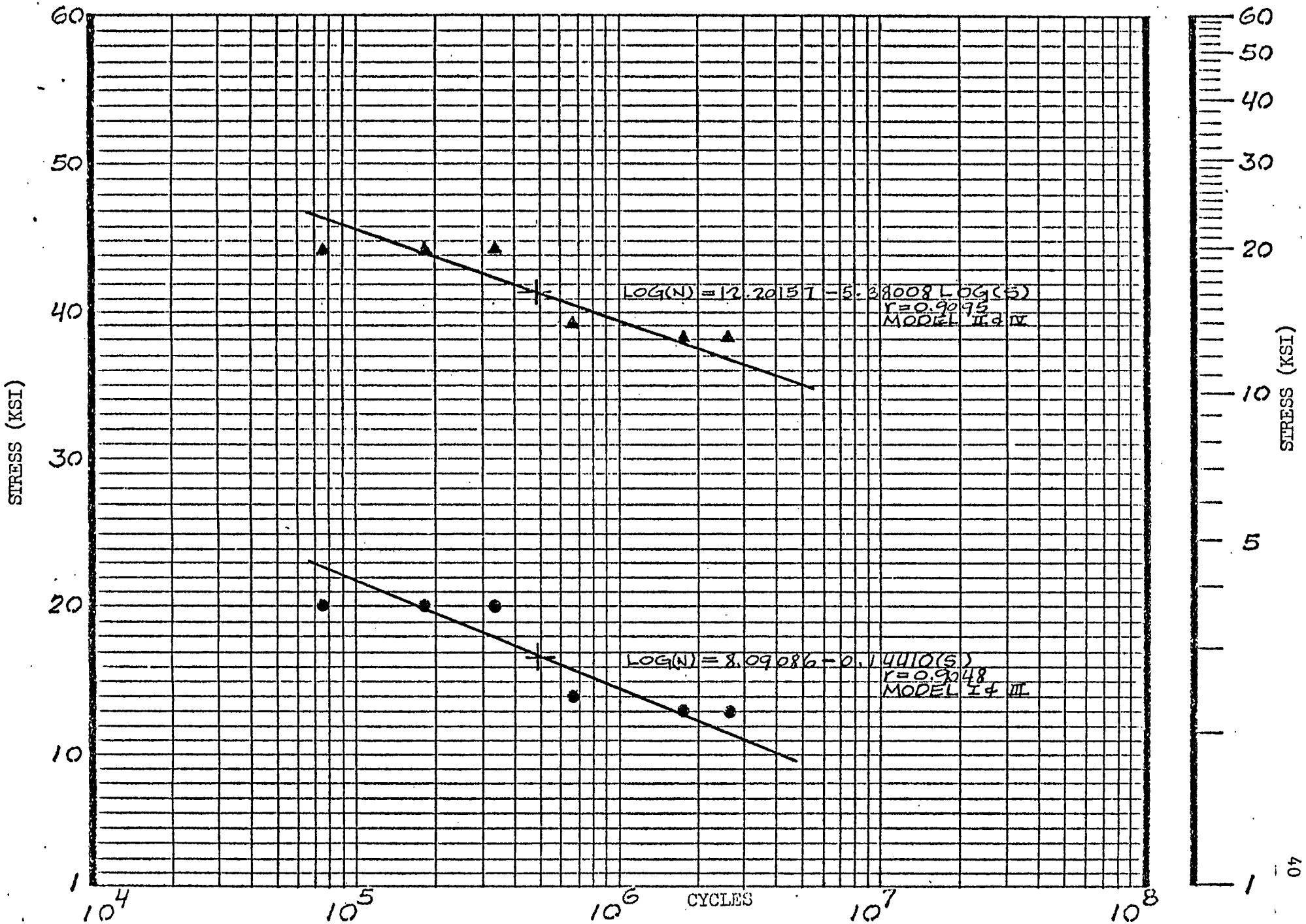

FIGURE 11 REGRESSION ANALYSIS FOR THE STEELP OF REFERENCE 22

$$\text{Log (N)} = 10.50744 - 4.27503 \text{ Log (S)} \quad (32)$$

Figure 10 (22) is for specimens of A-7 steel. As shown in the figure the semilog plot regression equation is:

$$\text{Log (N)} = 7.78599 - 0.1179 \text{ (S)} \quad (33)$$

The log-log equation is:

$$\text{Log (N)} = 11.21710 - 4.44398 \text{ Log (S)} \quad (34)$$

Figure 11 (22) is for specimens of steel P whose properties are given in Table 7. For the semilog plot:

$$\text{Log (N)} = 8.09086 - 0.14410 \text{ (S)} \quad (35)$$

The log-log equation is:

$$\text{Log (N)} = 12.20157 - 5.38008 \text{ Log (S)} \quad (36)$$

For the semilog plots the differences in slopes and the intersections of the mean regression lines with the abscissa were slightly different as seen in equations (31), (33) and (35). For the log-log plots greater differences are evident as both the slopes and the intersections of the mean regression lines with the abscissa varied as seen in equations (32), (34) and (36).

For judging the effect of central block width on fatigue strengths at two chosen lifetimes, see Table 8. The central block width of the specimens in Reference 21 was 0.875 inches; that for Reference 22 was 0.75 inches. That is, the central block widths were in the ratio: $\frac{w(\text{Ref. } 21)}{w(\text{Ref. } 22)} = \frac{0.875}{0.75} = 1.17$. Considering the two different steels and all of the models the fatigue strengths at 1×10^5 cycles of Reference No. 21 are from 4.10% to 30.7% smaller than those in Reference No. 22, while at 2×10^6 cycles the fatigue strengths of Reference No. 21 are from 28.87% to 42.22% smaller than those in Reference No. 22. This means that as the central block width increases, the fatigue strength

TABLE 7

STEEL PROPERTIES

Reference Number		Mechanical Properties Strength (ksi) Yield Pt.	UTS	Elong. %	Chemical Composition, percent C	Mn	P	S	Si
21	0.75 Pl	37.15	61.27	27.0	0.22	0.46	0.011	0.029	--
21	0.375 Pl	41.74	63.7	26.75	0.24	0.52	0.014	0.035	--
22	Steel A-7	33.3	57.4	33.0	0.17	0.68	0.016	0.039	0.03
22	Steel P*	56.8	76.7	25.0	0.12	0.56	0.106	0.043	0.32
23	0.75 Pl	43.0	70.2	29	0.17	0.82	0.013	0.035	0.25
23	0.375 Pl	41.2	63.5	32	0.16	0.94	0.012	0.016	0.50

*Additional chemical composition for Steel P:
Cu, 0.45%; Ni, 0.46%; Cr, 0.61%

TABLE 8

FATIGUE STRENGTH RATIOS AT CHOSEN LIFETIMES

Fatigue Strength (Ref. 22) A-7 Steel / Fatigue Strength (Ref. 21)	at 1×10^5 cycles (percent)	at 2×10^6 cycles (percent)
Model I and III	24.0/19.5 = 123.08%	12.8/9.0 = 142.22%
Model II and IV	25.5/19.5 = 130.76%	12.5/9.7 = 128.87%
Fatigue Strength (Ref. 22) Steel P / Fatigue Strength (Ref. 21)		
Model I and III	20.3/19.5 = 104.10%	12.6/9.0 = 140%
Model II and IV	22.0/19.5 = 112.82%	12.5/9.7 = 128.87%

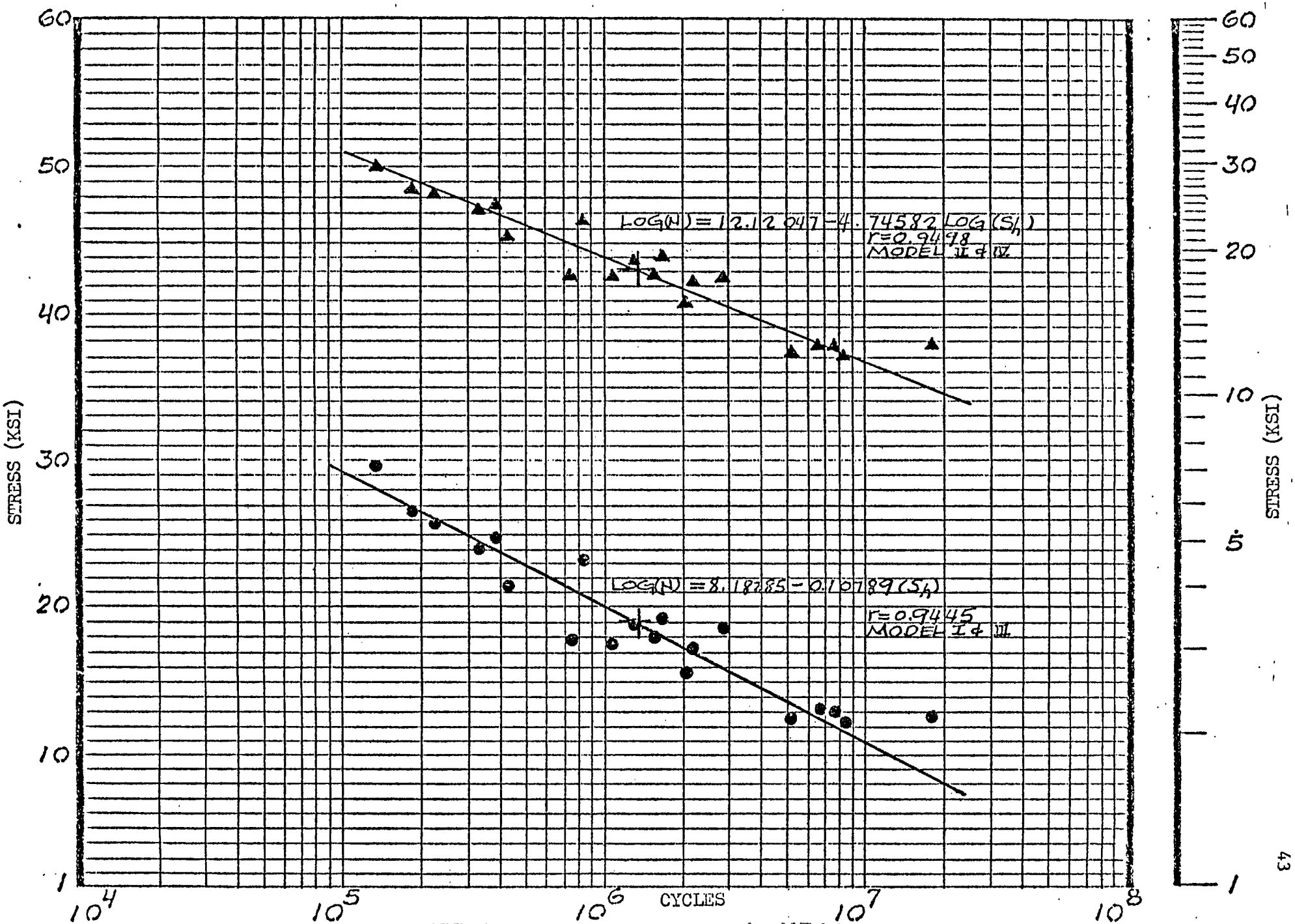

FIGURE 12 REGRESSION ANALYSIS FOR S_h OF REFERENCE 23

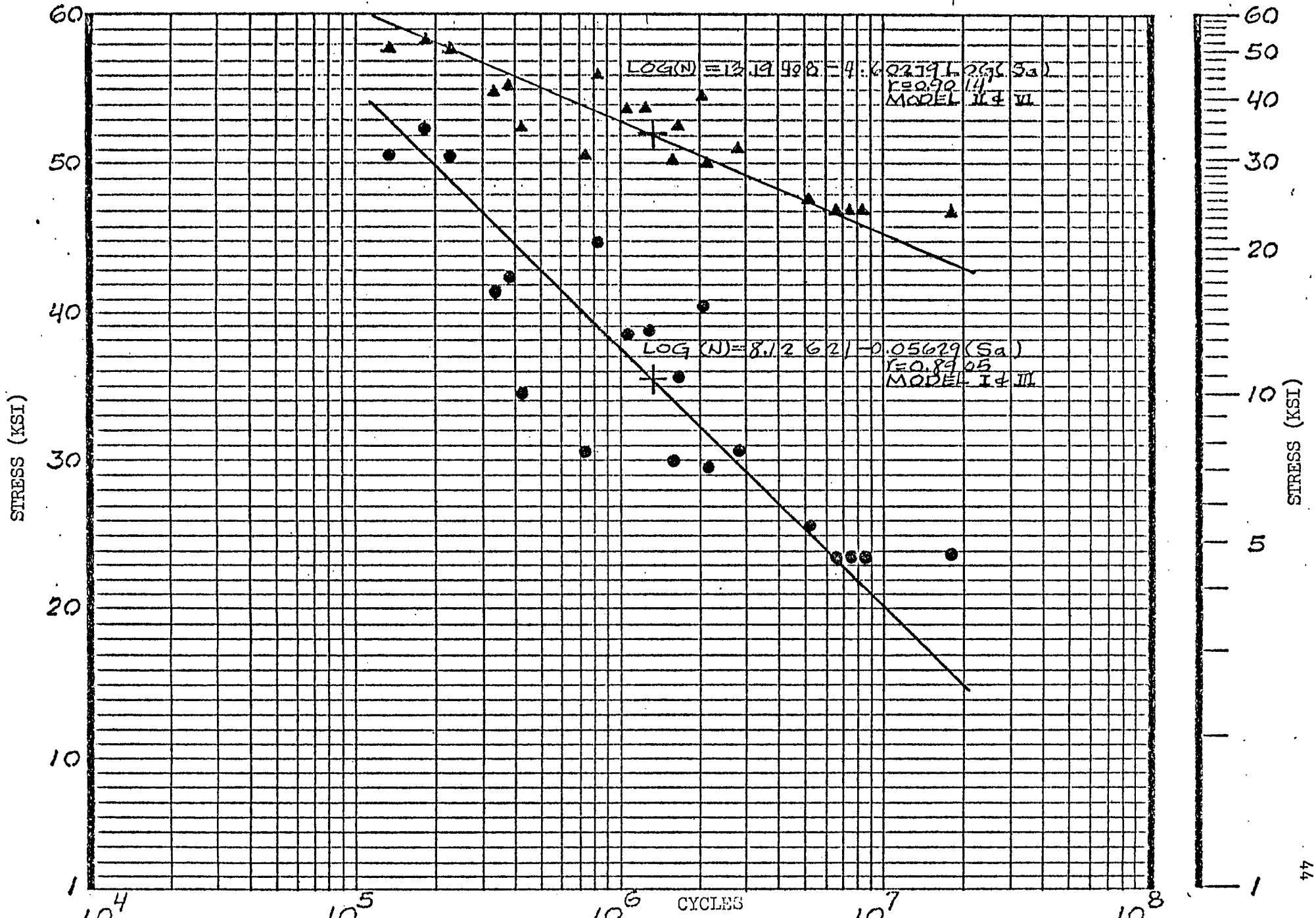

FIGURE 13 REGRESSION ANALYSIS FOR Sa OF REFERENCE 23

decreases. Thus, fatigue strength varies inversely with width of central block and with the type of steel, but in general the differences are small.

(2) The Effect of Length of Weld.

In this reanalysis test results were selected where three variables -- fillet weld size, main plate thickness, and central block width -- remained at constant levels while the length of weld varied. The two references used are numbers 22 and 23.

As before, mean regression lines were determined. The standard error of estimate varied from 0.194 to 0.282 for Reference 23, and from 0.273 to 0.338 for Reference 22. The correlation coefficient for each equation is shown in Figures 12 and 13. In Reference 23: stress S_h = P/2h x L); see Figure 14. The equations shown in Figure 12 are: for Models I and III

$$\text{Log (N)} = 8.18285 - 0.10789 \text{ (S)} \qquad (37)$$

and for Models II and IV

$$\text{Log (N)} = 12.12047 - 4.74582 \text{ Log (S)} \qquad (38)$$

Also in Reference 23, stress S_a = P/(2a x L); see Figure 14. The equations shown in Figure 13 are: for Models I and III

$$\text{Log (N)} = 8.12621 - 0.05629 \text{ (S)} \qquad (39)$$

and for Models II and IV

$$\text{Log (N)} = 13.19408 - 4.60279 \text{ Log (S)} \qquad (40)$$

The regression equations for Reference 22 are given in equations (33), (34), (35) and (36). As the welds in Reference No. 22 were of the partial penetration type, comparison should be made using equations (37) and (38). The applicable curves are shown in Figure 12 and Figures 10 and 11.

For the semilog plots the differences in slopes and the intersections of the mean regression lines with the abscissa were slightly different as seen in equations (37), (33) and (35). For the log-log plots greater differences are evident as both the slopes and the intersections of the mean regression lines with the abscissa varied as seen in equations (38), (34) and (36).

As shown in Figures 9, 10 and 12, the results of the regression analysis show that the log-log models have correlation coefficients larger than those of the semilog models. The log-log models provide the best fits to all of the test data.

For judging the effect of length of weld the ratios of relative fatigue strength at two chosen lifetimes are shown in Table 9.

The length of weld of the specimens in Reference No. 22 was 4.0 inches; that for Reference No. 23 was 1.18 inches. That is, the weld lengths were in the ratio: $\frac{L\ (\text{Ref. } 22)}{L\ (\text{Ref. } 23)} = \frac{4.0}{1.18} = 3.39$. The fatigue strengths at 1×10^5 cycles of Reference No. 22 are from 24.17% to 46.80% smaller than those in Reference No. 23, while at 2×10^6 cycles the fatigue strengths of Reference No. 22 are from 36.0% to 38.89% smaller than those in Reference No. 23.

This means as the length of weld increases, the fatigue strength decreases. The result is reasonable and expected. The reason is that fatigue failure usually starts at the surface. The additional surface area of a long weld increases the probability that defects will exist which will reduce the time for crack initiation and subsequent fatigue failure.

TABLE 9

FATIGUE STRENGTH RATIOS AT CHOSEN LIFETIMES

Fatigue Strength (Ref. 23) / Fatigue Strength (Ref. 22) A-7 Steel	at 1×10^5 cycles (percent)	at 2×10^6 cycles (percent)
Model I and III	29.8/24.0 = 124.17%	17.5/12.8 = 136.72%
Model II and IV	32.0/25.5 = 125.49%	17.0/12.5 = 136.0%
Fatigue Strength (Ref. 23) / Fatigue Strength (Ref. 22) Steel P		
Model I and III	29.8/20.3 = 146.80%	17.5/12.6 = 138.89%
Model II and IV	32.0/22.0 = 145.45%	17.0/12.5 = 136.0%

(3) The Effect of Main Plate Thickness

Increasing the thickness of the main plate causes the point of failure to move from the toe of the weld to some section within the weld itself, according to Macfarlane and Harrison (24). Extracted in Table 10 are the applicable test results.

Other investigations studied during the reanalysis confirm the conclusion just stated as to size effect on fatigue strength (25, 26). Additional general conclusions can be summarized as follows:

(a) Experimental observations show that for unnotched axial specimens, fatigue strength is independent of size. For notched specimens size affects fatigue strength under all stress conditions.

(b) Fatigue strength is reduced by an absolute increase in the dimensions of the test specimens; this reduction is particularly significant if stress concentrations are present.

(c) The fatigue crack is usually formed near some local defect or in places where there is a non-homogeniety in the metal. These defects are scattered at random throughout the mass of the metal and differ in size and quality. An increase in absolute dimensions increases the surface area which is subjected to fatigue stress. This increases the probability of various defects due to machining, internal defects, etc. These defects are regarded as the places where the fracture begins.

(4) The Effect of Fillet Weld Size.

Three references pertained to the effect of fillet weld size on fatigue strength (23, 27, 28). The test results of References 23 and 27 show that as weld penetration increases the fatigue strength also increases. No matter what type of beveling, see Figure Note for Table 6,

TABLE 10

EFFECT OF MAIN PLATE THICKNESS ON FATIGUE STRENGTH

OF FILLET WELDS FOR AXIAL LOADING

Original Designation	Main Plate Thickness t (in)	Fillet Weld Size S (in)	Central Block Width w (in)	Location of Failure and No. of Specimens in the weld	at weld toe	Fatigue Strength Stress in the weld (ksi) 1×10^5	2×10^6	Stress at Weld Toe (ksi) 1×10^5	2×10^6
TTN 3	0.3125"	0.5"	1.5"	---	6	---	---	39.2	23.07
TTN 2	0.5"	0.5"	1.5"	7	---	12.32	5.15	---	---

Reference: 24

as the size of the weld increases, the fatigue strength increases. Changing the beveling from $b = 0$ to $b = S$ changes the weld from partial to full penetration type. As the fatigue strength increases and the size of the weld increases, the location of failure will move from weld root to weld toe (27, 28).

There is a critical fillet size for a given plate thickness, below which failure occurs at the root of the weld and above which failure occurs in the base metal at the toe of the weld. The critical fillet size is also the optimum fillet size since further increases in fillet size produces no further improvement in fatigue strength. The critical fillet size has been found to obey the empirical expression:

$$\frac{2S}{t} = K \text{ (a constant)}$$

in which S = critical fillet size, t = plate thickness. Ouchida and Nichioka (27) suggest that for zero-to-tension axial loading $K = 2.0$. In their investigation, $K = 2.0$ for $t = 0.63$ inches, and $K = 1.75$ for $t = 1.26$ inches. The critical fillet size may be reduced by beveling the main plate. When failure occurs at the root of the weld, that is, where the main plate abutts the central block, increases in fatigue strength of 40-50% can be achieved by increasing the weld penetration by beveling the main plate.

D. TRANSVERSE NON-LOAD-CARRYING CRUCIFORM SPECIMEN

Five papers were reviewed (29 - 33). Pertinent variables for three of these are shown in Table 11.

(1) The Effect of Attachment Width.

Conclusions drawn from studying Reference No. 29 are:

(a) As the depth of the weld penetration decreases the magnitude

TABLE 11

VARIABLES OF THE TRANSVERSE NON-LOAD-CARRYING CRUCIFORM JOINTS

Reference Number	Fillet Weld Size (in) S	Main Plate thickness (in) t	Attachment width (in) w	Length of weld (in) L	Stress Ratio R
31	0.3125"	0.625"	0.625"	6.75"	-1
32	0.3125"	0.625"	0.25"	6.75"	-1
33	0.31" - 0.79"	0.87"	0.87"	3.15"	0

of the stress concentration factor at the root of the weld tends to increase. The stress concentration factor at the weld root is less than that at the weld toe. Hence the stress distribution at weld toe usually controls the fatigue failure.

(b) The two welds where each attachment fastens to the sides of the main plate serve as stress concentration regions; these effects are often largest at the transition from weld metal to parent metal.

(c) The stress concentration factor at the weld toe varies only slightly with the depth of weld penetration.

(d) The stress concentration factors at both the weld toe and the weld root tend to incrase with increasing attachment width.

The dependence of fatigue life on the stress concentration factor for structural steel is further documented from data obtained on beams having various attachments (30). The beams of Reference 30 were fabricated of A 441 steel and contained 0.25, 2.0, 4.0 and 8.0 inch attachment widths. Figure 15 shows that the allowable stress range at a given lifetime decreases as the attachment width increases. As the attachment width increased from 0.25 to 8.0 inches, the stress concentration factor increased from 2.42 to 3.15.

In summary, these two investigations seem to indicate that as the width of attachment increases, the stress concentration factor increases and the fatigue strength decreases.

In this category only two papers were available for statistical reanalysis of the effect of attachment width (31, 32). Test results were selected so that variation was allowed in attachment width while the other variables were held constant.

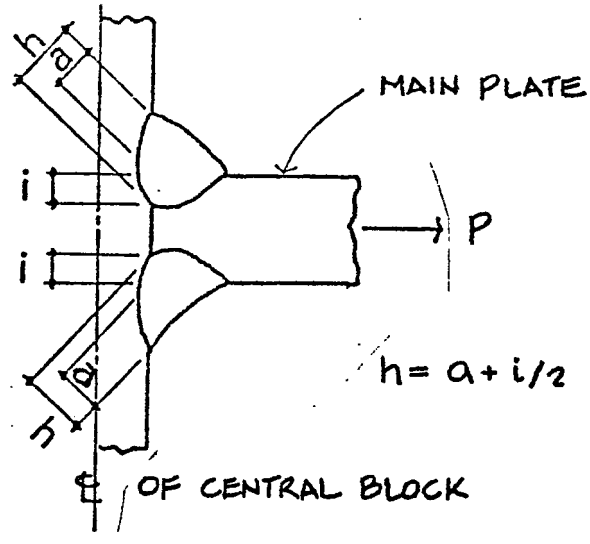

FIGURE 14 WELD DETAIL OF REFERENCE 23

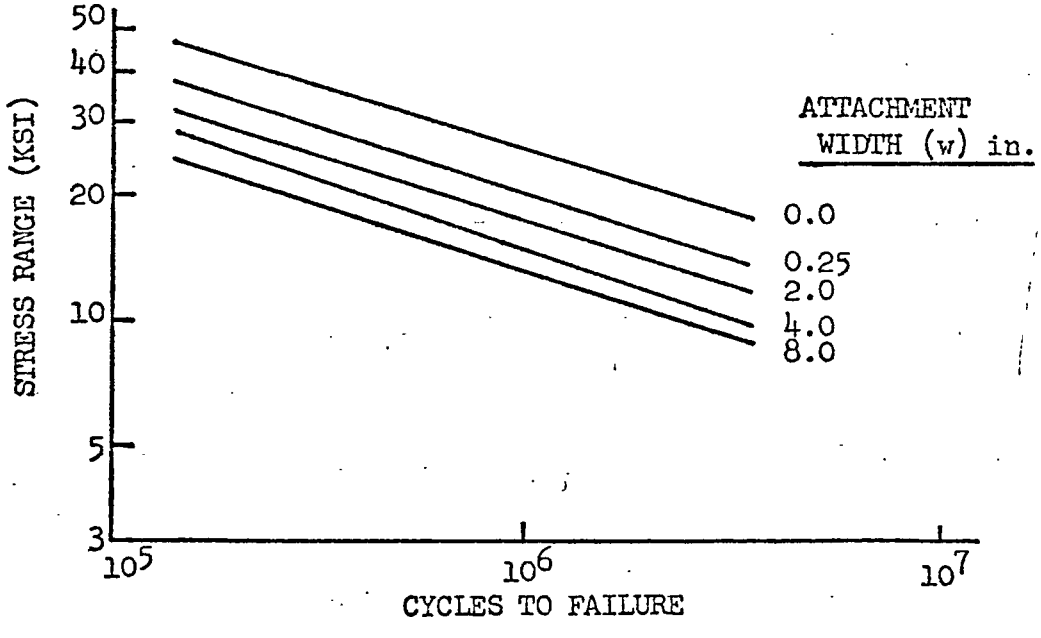

FIGURE 15 S-N CURVES FOR FLANGE ATTACHMENTS AND TRANSVERSE STIFFENERS (30)

The results of the statistical reanalysis are shown in Figures 16, 17, 18 and 19. The attachment width of the specimens in Reference No. 31 was 0.625 inches; that for Reference 32 was 0.25 inches. That is, the attachment widths were in the ratio: $\frac{w\ (\text{Ref. } 31)}{w\ (\text{Ref. } 32)} = \frac{0.625}{0.25} = 2.5$. Considering all of the models, the fatigue strengths at 2×10^5 cycles of Reference No. 31 are 19-26% larger than those in Reference No. 32. At 1×10^6 cycles the fatigue strengths of Reference No. 31 are 21-27% larger than those in Reference No. 32. This means that as the attachment width increases, the fatigue strength increases also. Thus, the result of the statistical reanalysis does not agree with the indications gained from References 29 and 30. The discrepancy is commented upon in the CONCLUSIONS.

(2) Fillet Weld Size.

Only the Ohta and Eguchi (33) paper was found to be useful in this category. Their conclusion was that with fillet size ranging from 0.31" - 0.79" the fatigue strengths at 1×10^5 cycles were from 34.41 ksi to 43.09 ksi; the fatigue strengths at 5×10^5 cycles were from 24.17 ksi to 28.01 ksi; the fatigue strengths at 2×10^6 cycles were from 16.50 ksi to 19.34 ksi. Thus the variation in fillet size does not have a large effect on fatigue strength of non-load-carrying joints at high cycle lifetimes. In general, for the same size fillet weld and identical specimen geometry, the fatigue strengths of specimens with non-load-carrying attachments are larger than those for specimens where the main member length is interrupted by a load carrying insert or block.

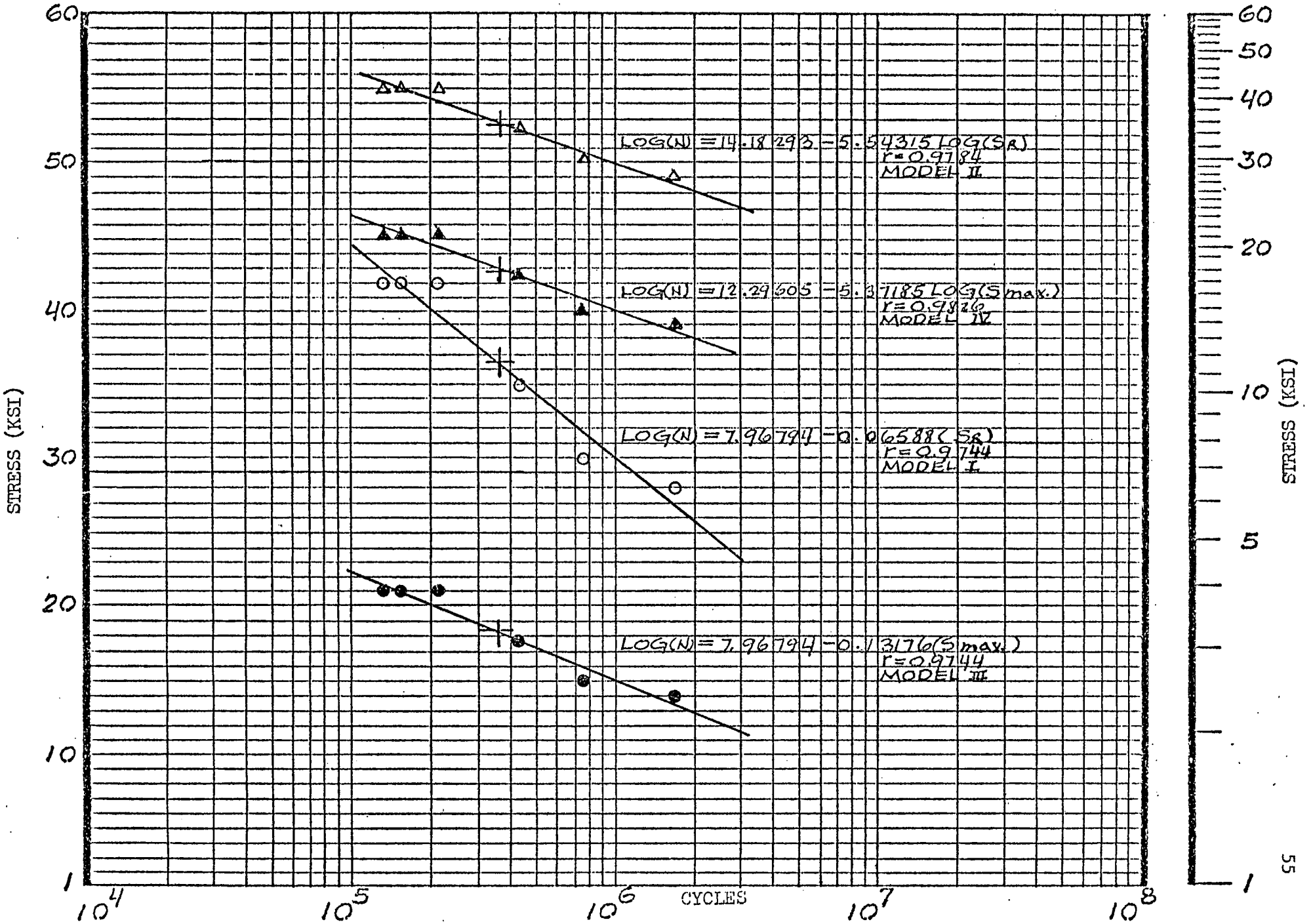

FIGURE 16 REGRESSION ANALYSIS FOR CARBON STEEL OF REFERENCE 31

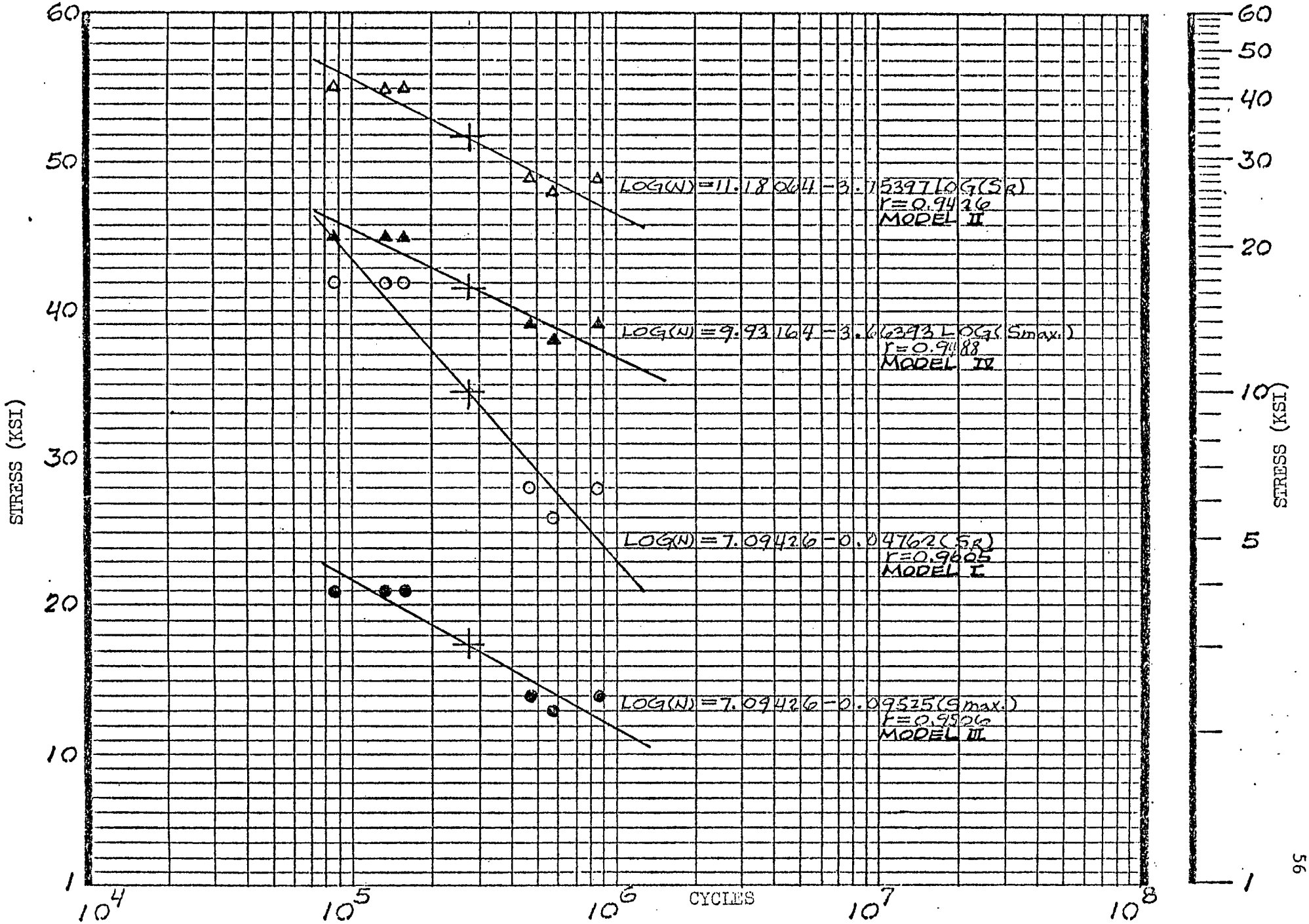

FIGURE 17 REGRESSION ANALYSIS FOR ALLOY STEEL OF REFERENCE 31

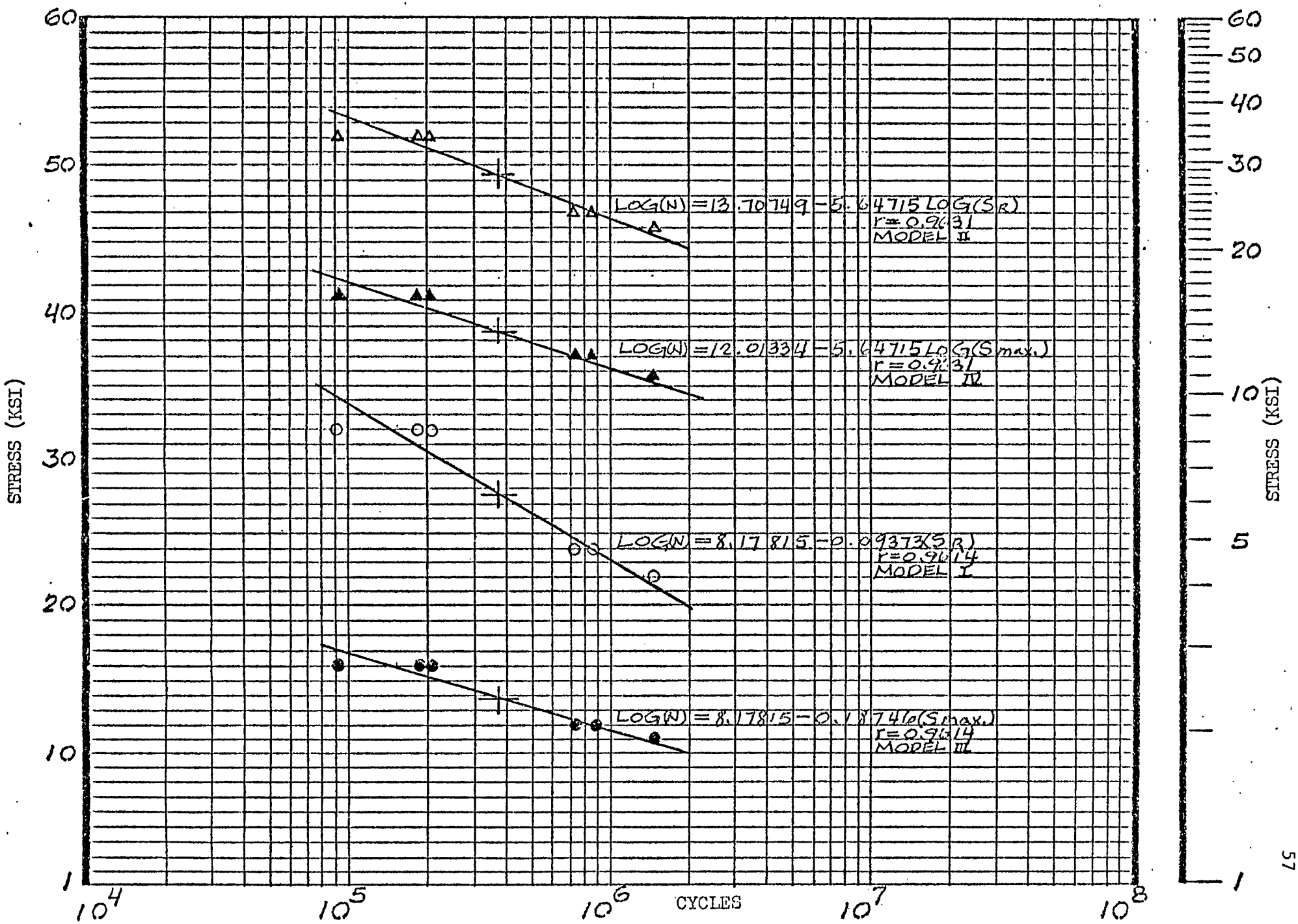

FIGURE 18 REGRESSION ANALYSIS FOR CARBON STEEL OF REFERENCE 32

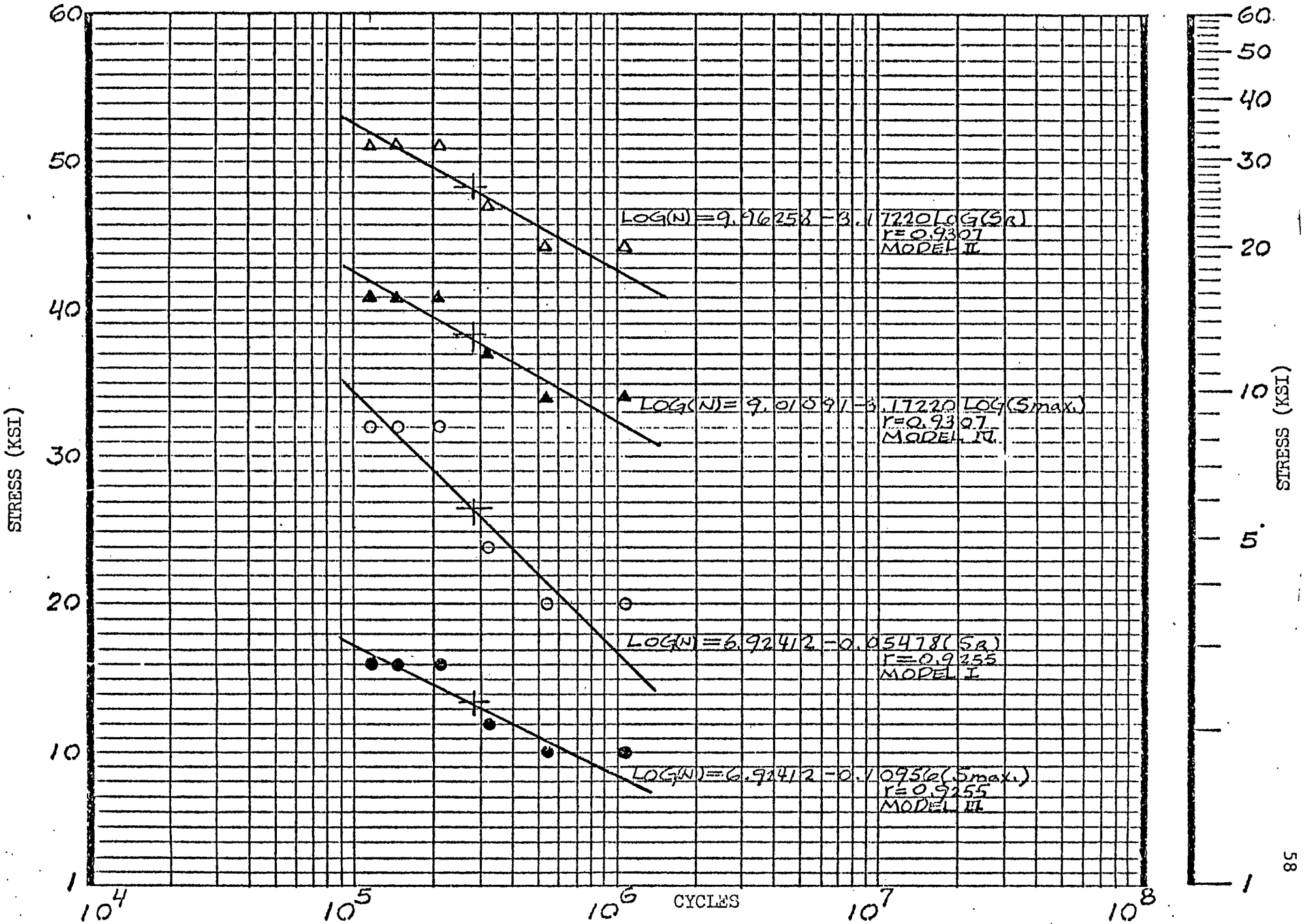

FIGURE 19 REGRESSION ANALYSIS FOR ALLOY STEEL OF REFERENCE 32

(3) Length of Weld.

While the reduction of fatigue life of continuous longitudinal fillet welds is due mainly to metallurgical notches (lack of fusion, porosity, shrinkage cracks, inclusions, laminations, etc.) the fatigue life of transverse fillet welds is affected by these and the detrimental effects of mechanical stress concentrators such as weld surface contour, undercutting, surface ripples, and lack of penetration. Some advocate for design purposes that fatigue strengths of transverse fillet welds should be estimated to be about half those for continous longitudinal fillet welds.

CHAPTER 5

CONCLUSIONS

AND

RECOMMENDATIONS FOR FUTURE WORK

A. CONCLUSIONS

1. As central block width increases for load-carrying cruciform joints the fatigue strength decreases. For non-load-carrying cruciform joints the data of several investigators do not agree. It is thought that as the attachment width increases the fatigue strength should tend to decrease.

2. For load-carrying cruciform joints, as the length of weld increases the fatigue strength decreases.

3. Fillet weld size has little effect on fatigue strength for both load-carrying and non-load-carrying cruciform joints.

4. Lack of weld penetration lowers the fatigue strength of transverse fillet welds.

5. The methodology used in this reanalysis could be applied to test results of other types of welded joints.

6. Thickness of the main plate has a singificant effect on the critical fillet weld size and the failure location.

7. The statistical method of analysis can be a continuing process and as additional experimental results become available, up-dated statistical reanalysis may be conducted.

B. RECOMMENDATIONS FOR FUTURE WORK

1. Fatigue life distribution at the fatigue limit.

If the metal has a very sharp turning point at the fatigue limit (the so-called knee point), or at stress levels a little bit above or a little bit below the fatigue limit, the fatigue problem turns out to be the determination of the fatigue life distribution around the knee

point. Previous works show that the location of the knee point, defined as the particular fatigue life at which the S-N curve flattens, will be a function of stress concentration factor, fatigue limit, ultimate tensile stress, and stress ratio. Trukyakov (5) reported the knee point for steel to be in the range between 1.5×10^6 and 3.5×10^6 cycles. Takahaski, et. al., (15) indicated that for as-rolled-surface specimens of steel the number of cycles at the knee point is about 1×10^6 smaller than that for plain machined specimens, and decreases linearly with an increase of tensile strength (UTS). There is a wide range of argument on the subject; the writer does not intend to discuss the various points of view here. Clarification of this in future investigations would be very beneficial.

2. Duration of tests.

It has become evident in recent years that the long-life fatigue behavior of welded joints for offshore industrial structures has become an important field for fatigue testing. The practice of discontinuing fatigue tests after two million applications of load should no longer be acceptable. Failures do occur after two million cycles and oftentimes offshore structures have lifetimes many times this figure.

3. Relationship between flat and tubular structures.

One of the major differences between the behavior of flat and tubular structures is the high stress concentration which can be developed in the latter. Stress concentration values as high as 24 have been recorded for welded tubular T joints. This may be compared with values in the range of 2 to 4 which have been reported for fillet welded

joints in flat plate specimens. In addition, severe stress gradients occur in tubular joints and it may be incorrect to assume that fatigue data which have been obtained using plate specimens are necessarily valid for tubular joints. In order to clarify this, further statistical analysis should be conducted as more up-dated data become available.

4. Effect of stress raisers.

Fatigue behavior in the vicinity of stress-concentration regions should be examined more fully in the future experimental studies. Actual stress distributions are sometimes quite different from the uniform distributions which are usually assumed to exist.

APPENDIX A

FATIGUE OF WELDED STRUCTURES

General

Today welding is being used extensively throughout many engineering industries, such as building construction, ship building, pressure vessels, highway and railway bridges, aircraft and spacecraft structures, offshore construction, etc. There are many important advantages to the use of welding (34). Some of these advantages are:

(1) A decrease in weight of the final structural member.

(2) Welded joints can develop their full moment resistance for both elastic and plastic design, leading to a more economical use of continuous structures.

(3) A saving in time, and consequently of money, since much less preparation is needed than for bolting.

(4) The ease of repairing or strengthening of old structures with a minimum of inconvenience.

(5) The design time is shortened since there is less detailing in the fabrication.

(6) Good appearance is obtained, leading to a greater architectural versatility.

(7) The noise of fabrication is kept at a low level.

Even though many of the advantages in favor of welding can hardly be disputed, at the same time it has to be recognized that from the point of view of fatigue a wide range of strength values may be obtained for different types of welds and joint configurations. In fact, under static loading conditions some types of welded joints are stronger than the parts or materials which they join together. However, the problems arise from the change in the properties of, or the introduction of

notches into, the parent metal. The indiscrimate specification of welding by designers and its use without a proper appreciation of its possible consequences has resulted in a large number of both brittle and fatigue failures.

The classifications of welded joints may be shown as follows:

(1) In terms of different position of weldments.

(a) Butt joint.

(b) Tee joint (or cruciform joint).

(c) Lap joint.

(d) Edge joint.

(e) Corner joint.

(2) In terms of the direction of the weld with respect to applied stress.

(a) Transverse

(b) Longitudinal.

(3) In terms of load-carrying or not.

(a) Load carrying.

(b) Non-load-carrying.

(4) In terms of applicable welds.

(a) Fillet weld.

(b) Plug weld.

(c) Slot weld.

(d) Groove weld.

(e) Spot (or tack) weld.

(f) Seam weld.

(g) Flange weld.

(h) Flash weld, etc.

In order to consider the influence of the weld geometry on the strength of the joint a simple illustration is given in Figure 20. The figure shows the distribution of stress flow lines through the connected plates. Figure 21 shows the kinds of relative movement one can expect in several types of joints.

The fatigue strength of welded structures subjected to repeated loading differs essentially from static strength of base metal in that the presence of the weld affects the value of permissible stress in the base metal. In fact, a welded joint is a discontinuity of variable magnitude, always lowering the fatigue strength of the structure. This is mainly caused by the stress concentration due to geometric discontinuity at the weld and by metallurgical inhomogeneity of the weld and nearby parent metal. This clearly indicates the importance of the type of joint and the external joint geometry (surface condition and configuration of the joint). The effect of internal geometry (weld quality and presence of defects) is generally significant only when the stress concentration at the joint is small, that is, when the weld bead is machined or removed.

The Results of Previous Work.

Previous research works have indicated some important fatigue features of welded joints. Some of these are:

(1) The general type of joint appears only to have an effect in terms of the direction of the weld with respect to the applied stress. At longer lives the difference is not as significant as that at shorter lives.

(2) In rolled structural plates and shapes the discontinuities may

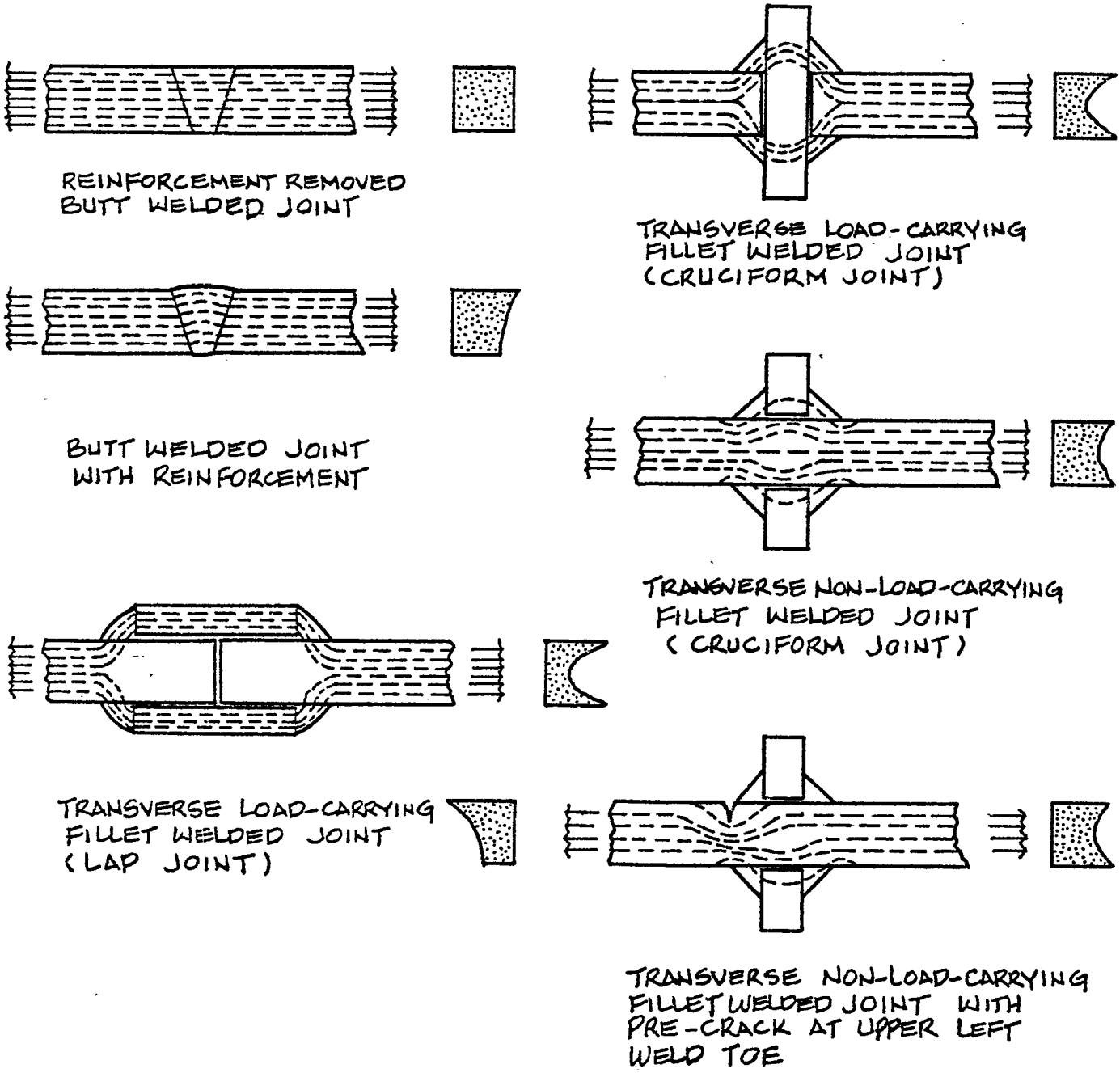

FIGURE 20 DETAILS OF STRESS FLOW LINES AND STRESS DISTRIBUTION DIAGRAMS FOR SOME COMMON FILLET WELDED JOINTS

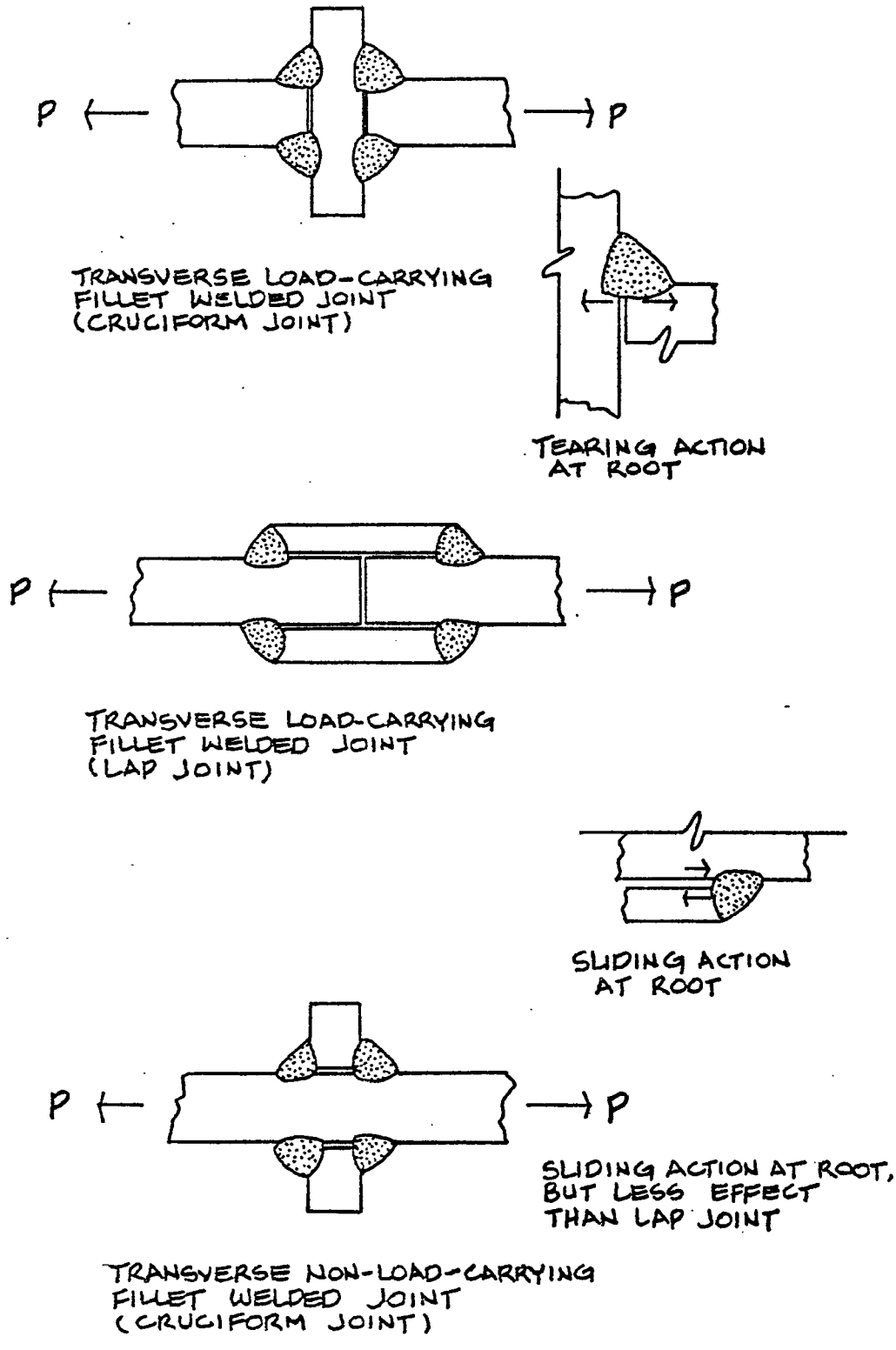

FIGURE 21 DETAILS OF RELATIVE MOVEMENTS AT WELD ROOT FOR THREE COMMON FILLET WELDED JOINTS

be in the form of surface imperfections, irregularities in mill scale, laminations, seams, and inclusions. Generally, laminations, seams, and inclusions have a microscopic thickness with respect to the direction of rolling. Although only indirectly related to the design of the connection, imperfections from the manufacturing or fabrication processes may affect fatigue life, depending on their location, size, and orientation with respect to the applied stress.

(3) In general, a discontinuity in a plane parallel to the line of applied stress will have little or no detrimental influence on the fatigue behavior and strength, and should be left alone. Attempts to remove them will usually result in a condition that is worse than the original discontinuity.

(4) When the dimension of an inclusion perpendicular to the line of stress is extremely small, the inclusion will have no detrimental effect on the behavior of the member. Sometimes the presence of inclusions situated parallel to the line of stress is beneficial as they serve to arrest the crack front if a crack should develop.

(5) In general, the initiation and growth of fatigue cracks will most likely occur in regions within the metal which are subjected to high tensile stresses and in which initial flaws exist. The higher the stress range and the larger the initial flaw, the faster the fatigue cracks propagate.

(6) In the broad definition of the nature of a defect, the following categories were intoduced by McEvily (35).

(A) Geometrical.

1) Undercut and cavity.

2) Overlap.

3) Poor fit-up, mismatch.

4) Excessive reinforcement (height and angle crown with surface).

5) Stress concentration in general.

6) Nature of weld dressing.

(B) Weld Character:

1) Lack of Penetration.

2) Lack of Fusion

3) Slag Inclusions.

4) Oxide films.

5) Delaminations.

6) Tungsten inclusion in GTA welds.

7) Gas porosity.

8) Microsegregation during cellular or dendritic growth.

9) Shape of weld puddle.

10) Arc strikes.

(C) Metallurgical.

1) Stress relief cracking.

2) HAZ hydrogen embrittlement (cold cracking)

3) Weld metal solidification cracking.

4) HAZ liquidation cracking (low melting point segregates).

5) Delamination of plate.

(D) Residual Stresses.

1) Constraint.

2) Repair welding.

(7) It has been shown in numerous investigations that stress range is the predominant variable affecting fatigue behavior of welded joints. Other stress variables, such as minimum stress, stress ratio, and maximum stress are not as significant for the purposes of design (36).

(8) The type of steel does not significantly affect the fatigue strength as long as stresses are below the yield point. In other words, for purposes of design it has been shown that the fatigue strength of a given welded detail is independent of the static strength of the parent material. In the German and Swedish Standards, however, high tensile steel structures can be designed to higher stresses in any case (36, 37).

(9) The new provisions or design rules are based essentially on the range of stress (the live load stress) and are independent of stress ratio, whereas in the old provisions fatigue strength varies with stress ratio. In this philosophy the fatigue design of a structure is based on the live load stress experienced by the member and welded joint; however, the maximum stress resulting from the dead-load plus live-load must also be considered in terms of the basic design stresses (38).

(10) Previous studies have indicated that weld details located in compression stress regions are not fatigue critical unless there is a possibility of some stress reversal. Cracks which form at a weld detail in a residual tensile stress region tend to adversely affect the member's load-carrying capacity, especially the fatigue capacity (36).

(11) The log-transformation of both cycle life and stress range results in a normal distribution of the test data at all levels of stress range, and a linear relationship between the two variables exists on the log-log plot. A theoretical stress analysis based on the fracture mechanics of stable crack growth confirms the suitability of

the log-log linear regression models that relate stress range and cycle life (36). This analysis showed that the primary factor causing variation in fatigue test data was the size of the initial micro-crack (36).

Probably the single most significant factor affecting the fatigue strength of a welded joint is the external geometry. The removal of reinforcement from the weld gives a marked rise in fatigue strength. The results are indicative only for good quality welds. For poor quality welds, the removal of reinforcement may simply shift the point of fracture initiation from the external notch to an internal notch (defect) without a significant increase in fatigue strength. Thus defects inherent to welds control the fatigue lifetimes. For "as welded" structures, a more realistic case, it is worth noting that geometrical factors may often be the overriding consideration, relegating other defect types to a minor role.

The present trend is to design for fatigue essentially on the range of applied stress because the level of mean residual tensile stress is usually high in the weld zone and the applied mean stress has little influence on fatigue life.

Stress Concentration Factor

Fatigue crack initiation in parent metal usually starts from notches, rounded regions, apertures, chamfers and other irregularities causing increases in the local stresses. These irregularities are important in the case of welded joints also because they create non-uniform distributions of stresses. In this case, however, in addition to the working stresses, residual stresses are also concentrated. The properties of the metal close to the weld undergo metallurgical change;

the stresses are intensified and redistributed in the concentration zones.

For a given weld geometry, the fatigue strength is ordinarily determined by the severity of the stress concentration at weld toe. With the weld reinforcement removed, the fatigue strength is determined by the stress concentration at the weld metal defects. The severity of a stress concentration, or "notch", is measured by the stress concentration factor, K_T, which is defined as the ratio of the maximum elastic stress in the region of the notch to the nominal stress in the member.

$$K_T = \frac{\sigma_{max.}}{\sigma_{nom.}} \quad \text{(For normal stress -- tension or bending)}$$

$$K_{Ts} = \frac{\tau_{max.}}{\tau_{nom.}} \quad \text{(For shear stress or torsion)}$$

Ductile materials, when subjected to static loads, are not as seriously affected by stress concentrations as are more brittle materials. This is due to the fact that ductile materials yield sufficiently to reduce the potentially high-stress concentration. When subjected to repeated loads, however, ductile materials fare only slightly better.

Various methods are employed to determine the stress concentration factor at an external discontinuity. Among them the most important ones are:

(a) Strain-gage method.

(b) Plaster-of-Paris method.

(c) Brittle-lacquer method.

(d) Photoelastic method.

(e) Fatigue method.

(f) Mathematical method.

Explanations of methods (a) through (d) can be easily located in any experimental stress analysis book. In recent years researchers have been concerned with using finite element analyses to determine the stress concentration factors for fillet weld toes and weld roots.

Method (e): When S-N curves are obtained for two series of fatigue specimens similar in every detail with the exception of a stress concentration, the ratio of the fatigue limits approximates the stress concentration factor. Because of the yielding of the material at the stress concentration, the value of K_T is smaller for the more ductile materials. The value of K_T is of real importance, however, for members subjected to repeated stress.

In this study only two specific types of welded joints were of interest. The two types are: (1) transverse non-load-carrying fillet welded joint, and (2) transverse load-carrying fillet welded joint. Both types of joint were limited to the cruciform shape only.

(1) Transverse Non-Load-Carrying Fillet Welded Joint (Cruciform)

Early experiments were conducted by Cherry (39) using photoelastic models, as shown in Figure 22, to determine the stress distribution and stress concentration factor. Cherry assumed that there was perfect homogeneity between the parent metal and the weld metal, and that there was perfect fusion and uniform bond strength throughout with no inital stress present. These assumptions were made for experimental purposes. Throughout the tests the thickness of the stressed member and the size and shape of the fillets were kept constant. The results of the

experiments on three different thicknesses of stressed member are shown in Figures 23, 24 and 25. Stress concentration factors obtained are correct both qualitatively and quantitatively.

From the stress concentration factors shown in Table 12 (a), (b) and (c) several conclusions can be drawn. These are discussed as follows:

The stress concentration factor at the weld toe is seen to be virtually independent of the depth of penetration of the weld when the attachment width is comparatively small but does depend on it to some extent when the attachments are thicker. The fact that having an attachment only to one side of the plate seems to give better results than having a pair attached opposite each other is almost certainly due to the beding effect introduced by the eccentric attachment. As a general rule, the stress concentration factors at both the toe and the root tend to increase with increasing attachment width.

Another investigation conducted by Navrotskii (29) gives similar results. For determining the stress in the section shown in Figure 28, that is A-A, B-B, and C-A, several wire resistance strain gages were attached at positions shown in Figure 27. The test specimens were tested under a tensile load of 108 ksi. The deformation was determined as being the average of the figures for two strain gages cemented onto opposite sides of the test specimens. An outline of the results is as follows:

(a) The two regions where each of the attachments fasten to the plate serve as stress concentration centers; these centers are located at the transition from the weld to the parent metal.

(b) It has been shown that the nature of fatigue behavior of the

TABLE 12

STRESS CONCENTRATION FACTORS IN MAIN MEMBERS DUE TO WELDED STIFFENERS (OR ATTACHMENTS)* (39)

Weld Penetrations in Inches	Stress Concentration Factors Root	Toe
(a) Attachment Width (or Stiffener Width) = 0.375"		
0.137	0.70	1.75
0.094	1.02	1.84
0.047	1.14	1.69
0.000	1.19	1.73
-0.020	1.21	1.75
-0.040	1.24	1.77
-0.80	1.38	1.67
-0.120	1.38	1.79
(b) Attachment Width = 1.0"		
0.500	0.69	1.87
0.250	1.14	2.01
0.125	1.38	2.24
0.000	1.64	2.56
-0.020	1.58	2.24
-0.040	1.72	2.60
-0.080	1.79	2.49
-0.120	2.01	2.49
(c) Attachment Width = 1.50"		
0.750	0.65	1.74
0.375	1.10	2.00
0.187	1.41	2.00
0.000	1.70	2.14
-0.020	1.70	2.32
-0.040	1.77	2.38
-0.080	1.88	2.54
-0.120	1.84	2.37

* Experimental data for the attachment welded on one side only was omitted from the tables shown above.

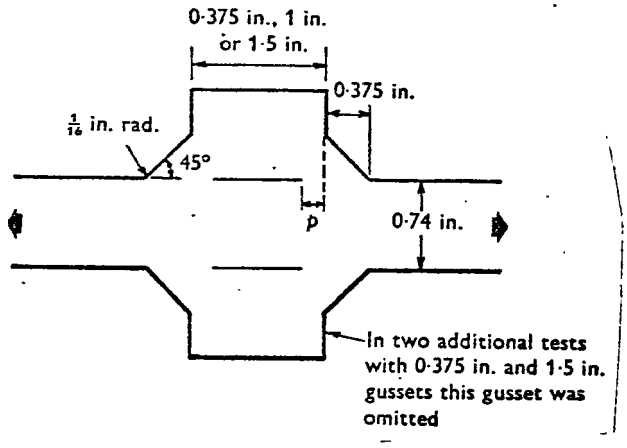

FIGURE 22 DETAILS OF PHOTOELASTIC SPECIMENS TESTED BY CHERRY (39)

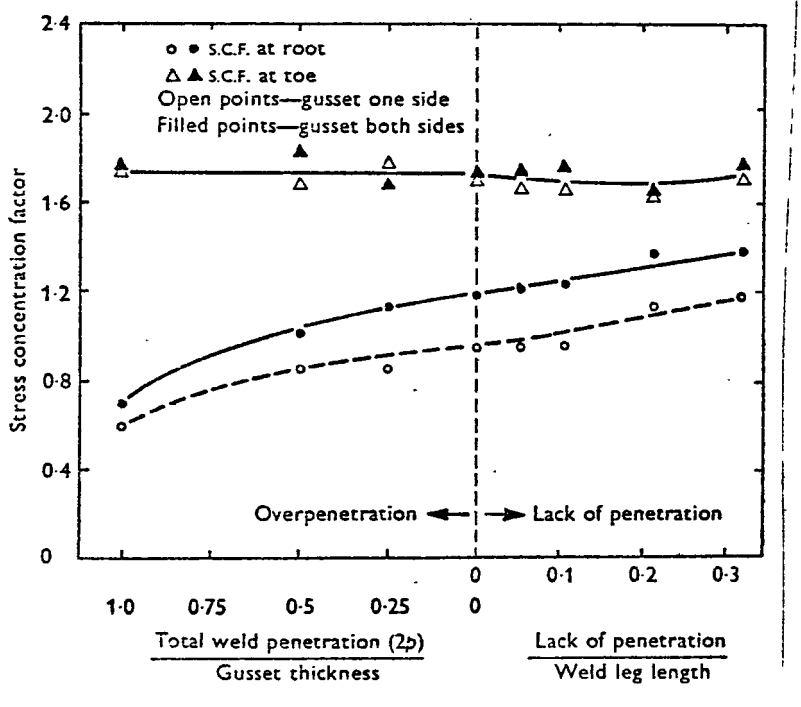

FIGURE 23 PHOTOELASTIC TEST RESULTS FOR SPECIMENS WITH 3/8" THICK GUSSETS. (OR ATTACHMENTS) (39) (37)

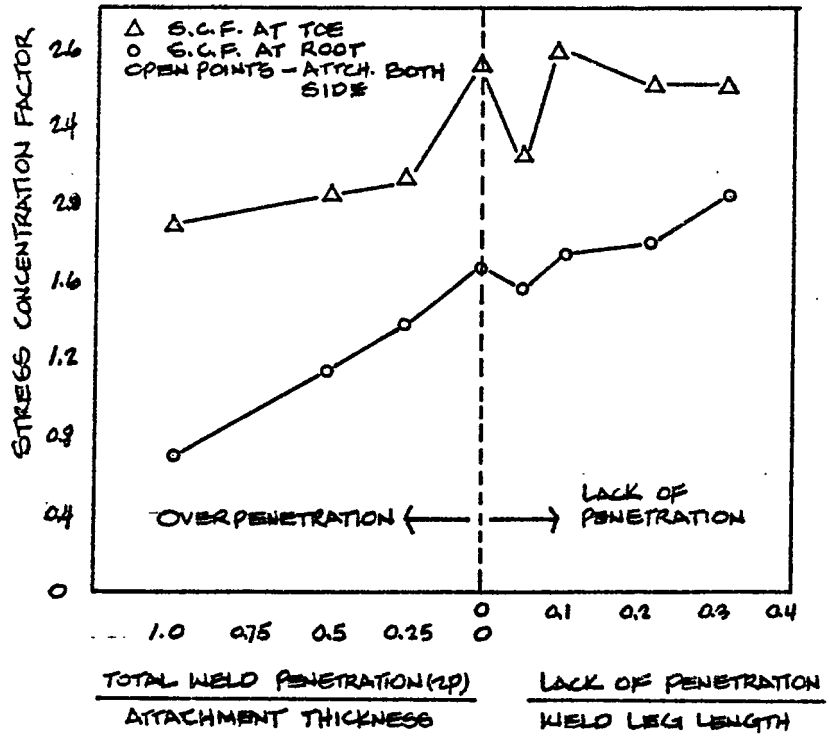

FIGURE 25 PHOTOELASTIC TEST RESULTS FOR SPECIMENS WITH 1.0" THICK ATTACHMENT. (39)

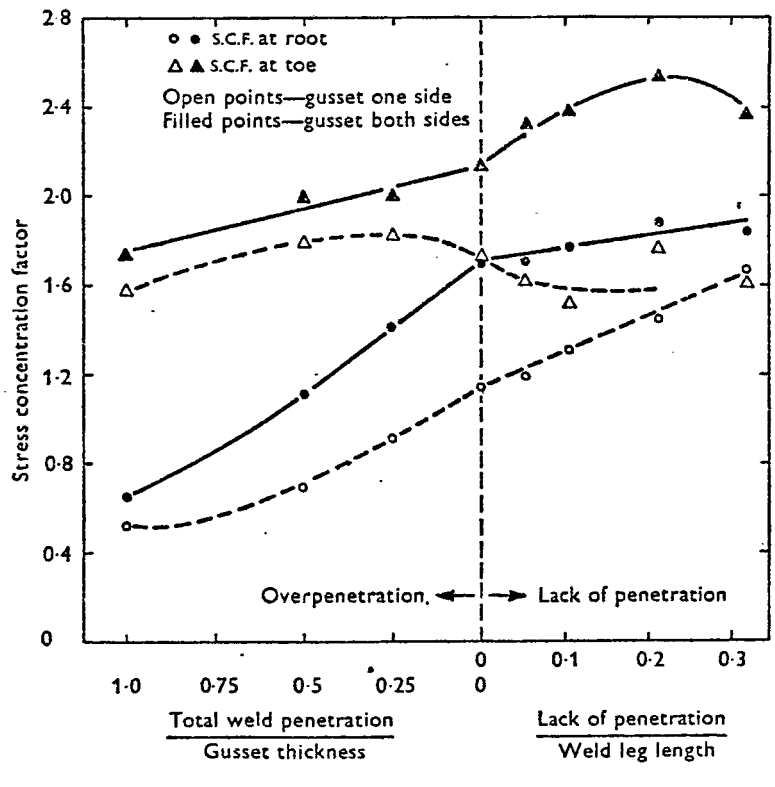

FIGURE 24 PHOTOELASTIC TEST RESULTS FOR SPECIMENS WITH 1.5" THICK GUSSETS (OR ATTACHMENTS) (39)(37)

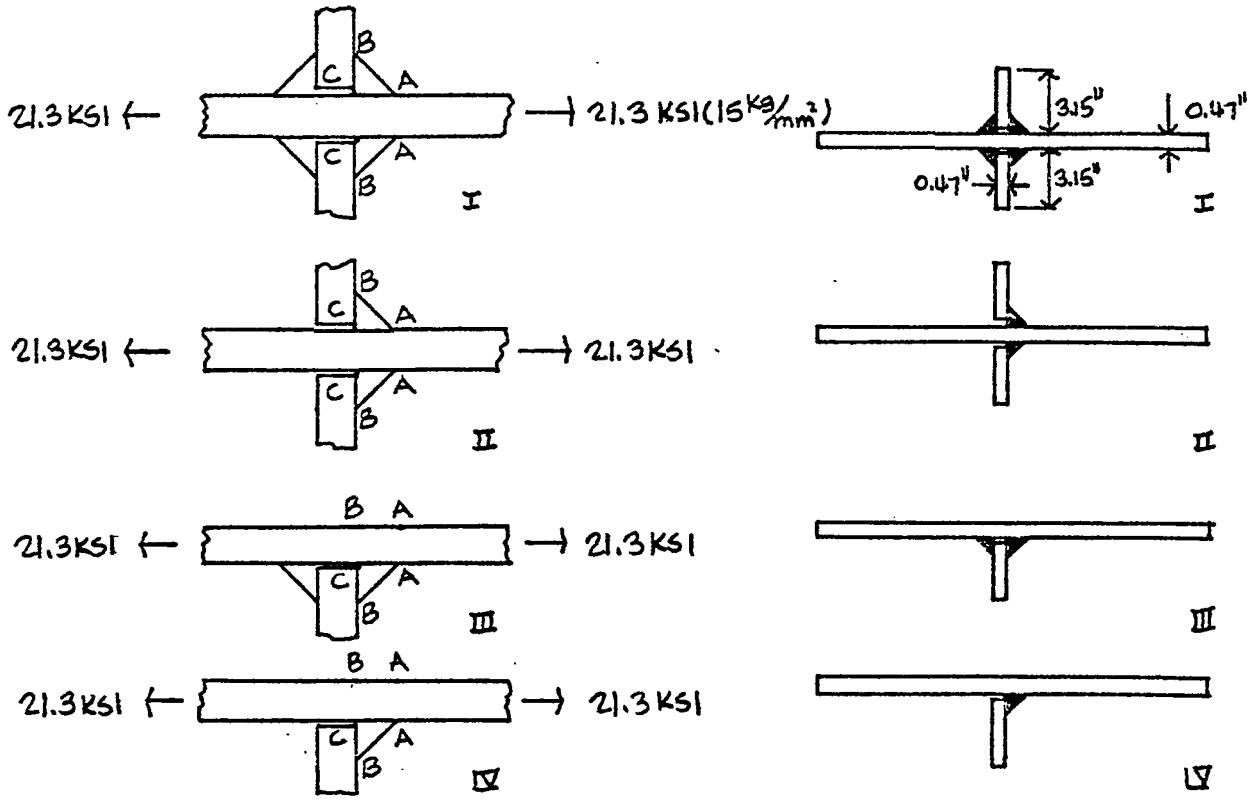

FIGURE 26 DETAILS OF SPECIMEN USING STRAIN GAGE METHOD TESTED BY NAVROTSKII (29)

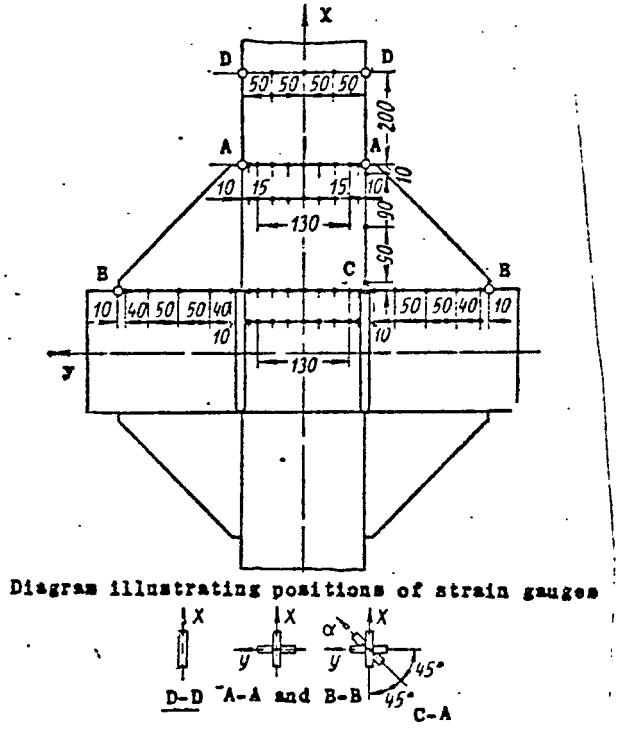

FIGURE 27 DIAGRAM OF THE SECTION, ALSO OF THE LOCATIONS OF STRAIN GAGES, FOR UNIT I.

test specimens depends on the design of assemblies containing stiffening attachments. All of the specimens of the series I and III tests where the weld beads were placed on both sides of the attachments, failed at the weld toe (or in Section A-A). The series II and IV test specimens, where the attachments had weld beads on only one side, started to fail at the weld root (or in Section B-B).

(c) Comparing Series I and III, in which weld beads were placed on both sides of the attachment, the reinforcement which forms greatly reduces the stresses in the regions at the weld toe. This means that the stress concentration factors at the weld roots are less than those at the weld toes. Hence, the stress distribution at the weld toe controls the failure.

(2) Transverse Load-Carrying Fillet Welded Joint (Cruciform)

Ouchida and Nishioka (27) reported that by using a photoelastic method the stress concentration factor, K_T, at the root of the weld joint, as shown in Figure 28, could be obtained. They considered that the throat area of each weld could be expressed as $(b + h) L$, where L is the width of fillet weld so that under axial loading the nominal stress on the critical section of the specimen through the weld throat could be defined as $P/[2 (b + h) \times L]$. They related the stress concentration factor at the weld root to $r/[2 (b + h)]$, where r is the radius at the tip of the slit corresponding to the root gap of the weld joint. Actually it represents the lack of penetration between the welds, this being maintained constant for all the tests. The conclusion from the tests may be outlined as follows:

(a) In the case of axial loading, as shown in Figure 29, it will

be seen that, as the C/r ratio decreases, the stress concentration decreases markedly; as the $r/[2(b + h)]$ increases, the stress concentration factor, K_T, decreases.

(b) Variable C which is the slit length between the welds, varies according to the different designs of the specimen.

(c) The r is constant, which is equal to 0.1 in. (0.25 mm), so it will be seen that, as $[2(b + h)]$ increases or $r/[2(b + h)]$ decreases, the stress concentration factor increases too. The $[2(b + h)]$ is twice that of the weld throat. In general, the stress concentration factor is proportional to the weld throat $(b + h)$ under axial loading.

(d) Under bending loads, see Figure 29, two variables, stress concentration factor K_T and $r/[2(b + h)]$ are proportional to each other. But variables K_T and $[2(b + h)]$ are inversely proportional to each other. The effect of either variable upon the other is not significant.

(e) The effect of the C/r ratio upon the stress concentration factor for the case of axial loading is much greater than the same effect under bending. If r is constant and the slit length C increases, then the stress concentration factor increases as length increases. The two are proportional to each other.

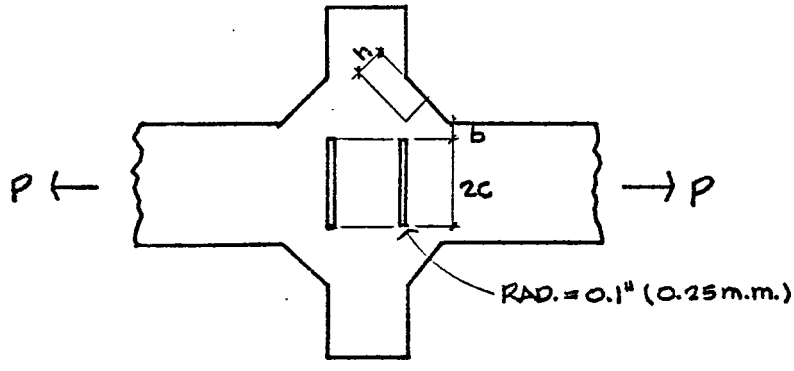

FIGURE 28 DETAILS OF SPECIMEN USED FOR AXIAL LOAD PHOTOELASTIC TESTS. (27)

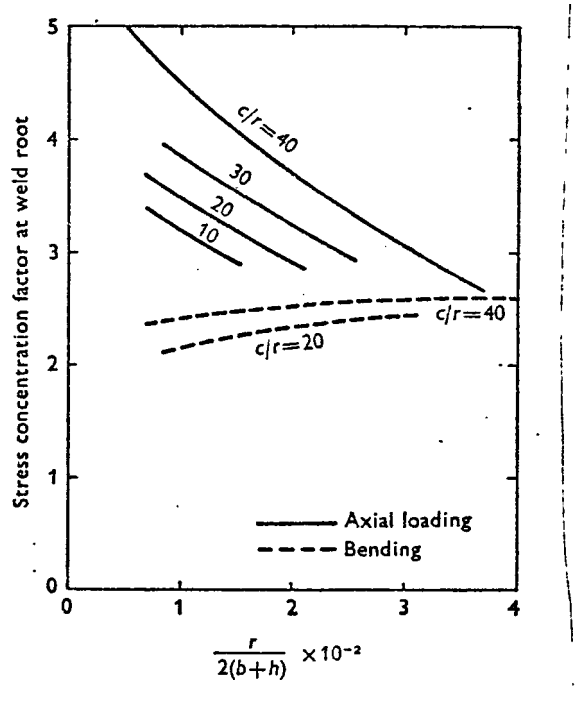

FIGURE 29 STRESS CONCENTRATION FACTOR AT WELD ROOT. (27)(37)

APPENDIX B

DETAILS OF STATISTICAL ANALYSIS

Regression Analysis:

Regression analysis is a method for establishing the functional relationship between two variables, where the variation in one measurement is considered while the other is held fixed. This relationship can be linear or non-linear.

Regression analysis, once a functional relationship between the dependent and the independent variables is established, can be used only to determine how the dependent variable changes with the independent variable. The analysis does not produce any information about why the changes occur.

A linear regression model is written in the general form

$$Y = B_0 + B_1 X_1 + B_2 X_2 + \cdots + B_K X_K + \varepsilon_i \qquad (41)$$

where Y is the dependent variable,

X_1 through X_K denote the independent variables,

ε_i denotes a random error component whose mean is zero and whose variance is σ^2

Ordinarily in fatigue analysis the two variables are stress S and life N (the independent and dependent variables, respectively). Also, it is usually assumed that for the finite fatigue life range the best results are obtained by fitting the data with a straight line on a log-log plot or on a semi-log plot. The equation for such a line is:

$$\log N = B_0 + B_1 \log (S) \qquad (42)$$

or

$$\log N = B_0 + B_1 (S) \qquad (43)$$

The regression can be applied to all distributions (normal, Weibull, exponential, etc.); however, the regression method assumes that

the error in the dependent variable is normally distributed. The method requires no assumption about the distribution of the independent variable.

The Least Square Regression Line:

In equations (42) and (43) let

$$Y = \log N$$

$$\left\{ \begin{array}{ll} X = \log S & \text{(log-log plot and semi-log plot, respectively)} \\ \text{or} \quad X = S & \end{array} \right.$$

The least square regression line of Y on X is

$$Y = a_0 + a_1 X \tag{44}$$

where a_0 and a_1 are fitted constants.

$$\Sigma Y = a_0 N + a_1 \Sigma X \tag{45}$$

$$\Sigma X Y = a_0 \Sigma X + a_1 \Sigma X^2 \tag{46}$$

where N = the number of $X - Y$ pairs which yield

$$a_0 = \sqrt{\frac{(\Sigma Y)(\Sigma x^2) - (\Sigma x)(\Sigma XY)}{N(\Sigma X^2) - (\Sigma X)^2}} \tag{47}$$

$$a_1 = \sqrt{\frac{N(\Sigma XY) - (\Sigma X)(\Sigma Y)}{N(\Sigma X^2) - (\Sigma X)^2}} \tag{48}$$

Standard Deviation

The standard deviation of a set of N numbers $X_1, X_2, \ldots, X_N$ is denoted by s and is defined by

$$s = \sqrt{\frac{\sum_{j=1}^{N} (X_j - \bar{X})^2}{N}}$$

$$= \sqrt{\frac{\Sigma (X - \bar{X})^2}{N}} = \sqrt{\frac{\Sigma x^2}{N}} \tag{49}$$

where x represents the deviations of each of the numbers X, from the

mean $\bar{X}$. Thus s is the root mean of the deviations from the mean or, as it is sometimes called, the root mean square deviation.

Some properties of standard deviation for normal distributions are:

(a) 68.27% of the cases are included between $(\bar{X} - s)$ and $(\bar{X} + s)$ (i.e., one standard deviation on either side of the mean).

(b) 95.45% of the cases are included between $(\bar{X} - 2s)$ and $(\bar{X} + 2s)$.

(c) 99.73% of the cases are included between $(\bar{X} - 3s)$ and $(\bar{X} + 3s)$.

Standard Error of Estimate:

If $Y_{est.}$ represents the value of Y for a given X as estimated from equation (44), a measure of the scatter about the regression line of Y on X is supplied by the quantity

$$S_{Y \text{ON } X} = \sqrt{\frac{\Sigma(Y - Y_{est.})^2}{N}} \qquad (50)$$

which is called the standard error of estimate of Y on X. See Tables 13 to 16 for numbers.

The standard error of estimate has properties analogous to those of the standard deviation. The standard error of estimate is the standard deviation of errors ε_i in Equation (41).

Correlation Coefficient:

The square of the sample correlation coefficient r is the best estimate of that fraction of the population Y variance accounted for by the regression on X (Please see Tables 13 to 16).

TABLE 13. STATISTICAL ANALYSIS OF REFERENCE 21

Model	B_0	B_1	Correlation coefficient, r	Standard error of estimate, S	F - ratio
I & III	7.36240	-0.12098	0.9299	0.2321	38.3360
II & IV	10.50744	-4.27503	0.9480	0.2009	53.1919

TABLE 14. STATISTICAL ANALYSIS OF REFERENCE 22

Model	B_0	B_1	Correlation coefficient, r	Standard error of estimate, S	F - ratio
A-7 Steel					
I & III	7.78599	-0.11719	0.8056	0.3382	12.9436
II & IV	11.21710	-4.44398	0.8162	0.3299	13.9681
Steel P					
I & III	8.09086	-0.14410	0.9048	0.2794	18.0594
II & IV	12.20157	-5.38008	0.9095	0.2727	19.1557

TABLE 15. STATISTICAL ANALYSIS OF REFERENCE 23

Model	B_0	B_1	Correlation coefficient, r	Standard error of estimate, S	F - ratio
$S_h = P/(2\ h \times L)$					
I & III	8.18285	-0.10789	0.9445	0.2033	148.7753
II & IV	12.12047	-4.74582	0.9498	0.1936	165.9469
$S_a = P/(2\ a \times L)$					
I & III	8.12621	-0.05629	0.8905	0.2816	68.9596
II & IV	13.19408	-4.60279	0.9014	0.2680	78.0343

TABLE 16. STATISTICAL ANALYSIS OF REFERENCE 31

Model	B_0	B_1	Correlation coefficient, r	Standard error of estimate, S	F - ratio
Carbon Steel					
I	7.96794	-0.06588	0.9744	0.1095	75.1098
II	14.18293	-5.54315	0.9784	0.1007	85.5303
III	7.96794	-0.13176	0.9744	0.1095	75.1098
IV	12.29605	-5.37185	0.9826	0.09057	111.6318
Alloy Steel					
I	7.09426	-0.04762	0.9506	0.1403	37.5036
II	11.18064	-3.75397	0.9426	0.1508	31.8849
III	7.09426	-0.09525	0.9506	0.1403	37.5036
IV	9.93164	-3.66393	0.9488	0.1428	36.0509

TABLE 17. STATISTICAL ANALYSIS OF REFERENCE 32

Model	B_0	B_1	Correlation coefficient, r	Standard error of estimate, S	F - ratio
Carbon Steel					
I	8.17815	-0.09373	0.9614	0.1440	48.8604
II	13.70749	-5.64715	0.9631	0.1409	51.2353
III	8.17815	-0.18746	0.9614	0.1440	48.8604
IV	12.01334	-5.64715	0.9631	0.1409	51.2353
Alloy Steel					
I	6.92412	-0.05478	0.9255	0.1510	23.8682
II	9.96258	-3.17220	0.9307	0.1458	25.8763
III	6.92412	-0.10956	0.9255	0.1510	23.8682
IV	9.01091	-3.17220	0.9307	0.1458	25.8763

$$r^2 = (a_1)^2 \frac{N\Sigma(X)^2 - (\Sigma X)^2}{N\Sigma(Y)^2 - (\Sigma Y)^2} \tag{51}$$

The sample correlation coefficient r varies from + 1 to - 1. If r is either + 1 or - 1, all observed X - Y pairs fall on the straight line described by Equation (44). The sign of r indicates a positive or negative slope a_1. If a is 0, the regression on X explains nothing about the variation in Y and the regression line is horizontal.

F - ratio

This measure is dependent on the ratio of the mean square deviation due to the regression to the mean square due to error. The F - ratios are compared with tabulated F - ratios for a level of significancne of α. A calculated F - ratio greater than the tabulated value means that, with a risk of α, one may state that the variable being tested has a significant effect on the fatigue life of the specimen.

BIBLIOGRAPHY

BIBLIOGRAPHY

1. Committee on Fatigue, "A Guide for Fatigue Testing and The Statistical Analysis of Fatigue Data," ASTM, STP No. 91-A, Second Edition, 1964.

2. Gurney, T. R. and Maddox, S. J., "A Re-analysis of Fatigue Data for Welded Joints in Steel," The Welding Institute Research Report, E/44/72, 1972.

3. Crooker, T. W., "Basic Concepts for Design Against Structural Failure by Fatigue Crack Propagation," NRL Report 7347, Jan. 13, 1972.

4. Fisher, J. W., Frank, K. H., Hirt, M. A., and McNamee, B. M., "Effect of Weldments on The Fatigue Strength of Steel Beams," NCHRP Report No. 102, 1970.

5. Trufyakov, V. I., "Problems in the Procedure for Fatigue Tests on Welded Joints," Avt. Svarka., 1963, No. 1, pp. 1-8.

6. Grover, H. J., "Fatigue of Aircraft Structures", NAVAIR 01-1A-13, 1966.

7. Freudenthal, A. M., "Aspects of Cumulative Damage in Fatigue Design," AFML-TR-67-112, Air Force Materials Laboratory, Wright-Patterson Air Force Base, Ohio, April 1967.

8. Madayag, A. F., Editor, Metal Fatigue -- Theory and Design, John Wiley & Sons, Inc. 1969.

9. Yamaguchi, I., Terada, Y., and Nitta, A., "On the Fatigue Strength of Steels for Ship Structures", IIW Doc. XIII-425-66, 1966.

10. Weibull, W., Fatigue Testing and Analysis of Results, Pergamon Press, 1961.

11. Lipson, Charles, and Sheth, N. J., Statistical Design and Analysis of Engineering Experiments, McGraw-Hill Book Co., 1973, p. 518.

12. Broch, J. T., "On the Damaging Effects of Vibration," B & K Technical Review, No. 4, 1968.

13. Moses, F., and Garson, R., "New Procedure for Design of Highway Bridge Girders," Transportation Research Record No. 507, 1974.

14. Reemsnyder, H. S., "Procurement and Analysis of Structural Fatigue Data," J. Struct. Div., ASCE, Vol. 95, No. ST 7, July 1969.

15. Takahashi, K., et. al., "Fatigue Strength of High Tensile Structural Steels and Welded Joints," Bulletin of the JSME, Vol. 16, No. 92, Feb. 1973.

16. White, D. J. and Lewszuk, J., "Cumulative Damage in Push-Pull Fatigue of Fillet Welded Mild Steel Plate Subjected to Narrow Band Random Loading," Proc. I. Mech. E., Vol. 185, 28171, 1971.

17. Fisher, B. C., and Sherratt, F., "Random Load Fatigue Damage Accumulation in Mild Steel," Proc. I. Mech E., Vol. 187, 22/73, 1973.

18. Munse, W. H., and Grover, L. M., "Fatigue of Welded Steel Structures," Welding Research Council, 1964.

19. SAE Iron & Steel Technical Committee, Fatigue Design Handbook -- A Guide for Product Design and Development Engineers, SAE, 1968.

20. Basquin, O. H., "The Experimental Law of Endurance Tests," Proc. ASTM, Vol. X, 1910.

21. Wilson, W. M., Munse, W. H., and Bruckner, W. H., "Fatigue Strength of Fillet-weld, Plug-weld, and Slot-weld Joints Connecting Steel Structural Members," University of Illinois Engineering Experiment Station, Bulletin No. 380, May 1949.

22. Stallmeyer, J. E., et. al., "Fatigue Strength of Welds in Low-Alloy Structural Steels," Welding Research Supplement No. 16, 1956, pp. 298-307S.

23. Hoisveen, S., and Persson, H. A., "Influence of Penetration on Fatigue Strength of Fillet Welds Made Automatically by Co_2 and Submerged Arc," Svetsen, Vol. 22, No. 3, 1963, pp. 75-80. Also, Welding Research Abroad, Vol. 9, No. 10, 1963, pp. 10-14.

24. Macfarlane, D. S., and Harrison, J. D., "Some Fatigue Tests of Load Carrying Transverse Fillet Welds," British Welding Journal, Vol. 12, 1965, pp. 613-23.

25. Kravchenko. P. Ye., Fatigue Resistance, translated from Russian by O. M. Blunn, Pergamon Press, 1964, page 112.

26. Forrester, E. R., and Thevenow, V. H., "Designing For Expected Fatigue Life," Proceedings of ASME Reliability and Maintainability Conference, San Francisco, C lif., July 14-17, 1968.

27. Ouchida, K., and Nishioka, A., "A Study of Fatigue Strength of Fillet Welded Joints," International Institute of Welding Doc. XIII-338-64, 1964.

28. Inoue, H., "Fatigue Strength of Fillet Welded Joints of Oblique Crossing Member," Proceedings of Japan - U. S. Seminar, 1973, Tokyo, Japan, pp. 235-247.

29. Navrotskii, E. E., and Lavochkin, G. V., "Determination of the Stresses at Points Where Transverse Stiffening Ribs Are Welded On," Svar. Proiz., 1963, No. 5, pp. 1-5.

30. Fisher, J. W., et. al., "Fatigue Strength of Steel Beams with Welded Stiffeners and Attachments," NCHRP, Report No. 147, 1974.

31. Wilson, W. M., et. al., "Fatigue Tests of Welded Joints in Structural Steel Plates," University of Illinois Engineering Experiment Station, Bulletin No. 327, 1941.

32. Wilson, W. M., et. al., "Fatigue Strength of Fillet-weld and Plug-weld Connections in Steel Structural Members," University of Illinois Engineering Experiment Station, Bulletin No. 350, 1944.

33. Ohta, S., and Eguchi, Y., "Fatigue Strength of 80 kg/mm^2 High Tensile Strength Steel Plates with Transverse Fillet Welded Attachments," Trans. Japanese Welding Society, Vol. 3, No. 2, Sept. 1972, pp. 9-16.

34. Tall, L., Editor, Structural Steel Design, 2nd Edition, The Ronald Press, 1974.

35. McEvily, A. J. Jr., "On the Role of Defects in Crack Initiation in Welded Structures," Proc. of the Japan - U. S. Seminar, Tokyo, Japan, 1973, pp. 96-104.

36. Fisher, J. W., Albrecht, P. A., Yen, B. T., Klingerman, D. J., and McNamee, B. M., "F tigue Strength of Steel Beams with Welded Stiffeners and Attachments," NCHRP Report No. 147, 1974.

37. Gurney, T. R., Fatigue of Welded Structures, Cambridge University Press, 1968.

38. Munse, W. H., "Fatigue of Welded Structures -- Conf. held by the Welding Institute, July 6-9, 1970, The Changing American Fatigue Design Specifications, 1970.

39. Cherry, W. R., "Stress Concentration Factors in Main Members Due to Welded Stiffeners," Master's Thesis, Oregon State College, June, 1942, also, Welding Journal, Vol. 20, No. 12, 1941.